universität wien

DIPLOMARBEIT

DIPLOMA THESIS

Linking viruses to their prokaryotic hosts in deep waters of the northeastern subtropical Atlantic Ocean

Thomas Griessler

angestrebter akademischer Grad:

Magister der Naturwissenschaften (Mag. rer. nat.)

Wien, 2012

Studienkennzahl lt. Studienblatt:	A 439
Studienrichtung lt. Studienblatt:	Diplomstudium Zoologie
Betreuer:	Univ.-Prof. Dr. Gerhard J. Herndl

TABLE OF CONTENTS

EINLEITUNG

Die Bedeutung von Mikroorganismen und Viren in den Meeren

Bereits in der zweiten Hälfte des 20. Jahrhunderts wusste man, dass relativ hohe Zahlen von Prokaryoten in den Weltmeeren vorkommen (Waksman und Renn, 1934; ZoBell, 1946), jedoch wurden diese Zahlen um ca. 3 Größenordnungen unterschätzt. Die Abweichungen der Zählungen entstanden aufgrund der Tatsache, dass diese nur kultivierbare Mikroorganismen berücksichtigten, die meisten Prokaryoten sind jedoch nicht kultivierbar (Hugenholtz, 2002). Man spricht in diesem Zusammenhang auch von der "Great plate count anomaly" (Staley und Konopka, 1985). Bis in die 1970er Jahre nahm man an, dass Prokaryoten lediglich Verwerter organischen Materials sind und nicht nennenswert zu biogeochemischen Kreisläufen beitragen. Diese Ansicht änderte sich in den 1980er Jahren, als Azam et al. (1983) den Begriff des „microbial loop" prägten. Damit ist gemeint, dass Prokaryoten gelöstes, organisches Material (engl. dissolved organic carbon = DOC) aufnehmen und damit die Basis der Nahrungskette schaffen. Ciliaten und Flagellaten fressen wiederum die Prokaryoten und machen das organische Material für höhere trophische Ebenen verfügbar (Figure 1). Da das DOC zum größten Teil von Organismen, die selbst Teil dieser Nahrungskette sind, stammt, beschreibt der Begriff „microbial loop" treffend den Kreislauf des DOC innerhalb dieser Nahrungskette bzw. Nahrungsnetzes (Figure 1). DOC kann von unterschiedlichen Quellen stammen, z. B. Ausscheidungen von Phytoplankton, sinkendes, zerfallendes Plankton, Exkretionsprodukte, „sloppy feeding" von Zooplankton, und – wichtig für diese Diplomarbeit – lysis durch Viren (Dafner und Wangersky, 2002).

Die ersten Erkenntnisse, dass Prokaryoten in hohem Maße von Viren infiziert sein und damit eine wichtige Rolle in aquatischen Systemen spielen können, wurden in den späten 1980er Jahren gemacht (Sieburth et al., 1988; Bergh et al., 1989; Proctor und Fuhrman, 1990). Als entdeckt wurde, dass durch Viren eine ähnlich hohe Mortalität wie durch Protisten verursacht wird (Fuhrman und Noble, 1995), war der Einfluss von Viren auf Prokaryoten bestätigt. Heute weiß man, dass das Sterben von Prokaryoten aufgrund viraler Infektion eine große Bedeutung für den Kohlenstoffkreislauf in aquatischen Systemen hat (Wommack und Colwell, 2000; Suttle, 2005 und 2007). Ein wichtiger Punkt ist, dass Viren Prokaryoten „lysieren", d. h. zerstören, aber nicht essen (trotz ihres Namens „Bakteriophagen"). Durch diese Lysis werden Prokaryoten in organisches Material konvertiert, welches wiederum verfügbar für andere Prokaryoten ist. Dieser „Kurzschluss" innerhalb des microbial loop wird „viral shunt" genannt (Figure 2) (Wilhelm und Suttle, 1999; Suttle, 2005). Geschätzte 20 % der Prokaryoten tragen daher statistisch gesehen niemals zum

Kohlenstoffffluss innerhalb der Nahrungskette bei, da sie von Viren lysiert werden, bevor sie von Protisten gefressen werden können (Wommack und Colwell, 2000).

Eigenschaften von Viren

Viren sind mit einer Anzahl von 10^{29} (Suttle, 2007) die zahlreichsten biologischen Einheiten in den Weltmeeren. Obwohl sie winzig sind (ca. 20–400 nm, La Scola et al., 2003) würden alle in den Meeren vorkommende Viren aneinandergereiht ein Band mit einer Länge von 10 Millionen Lichtjahren ergeben (Suttle, 2005 und 2007). Viren verfügen über unterschiedliche „Überlebens"-strategien, die bekanntesten sind der lytische und der lysogene Zyklus (Weinbauer, 2004; Suttle, 2007). Der lytische Zyklus führt zur Lysis der Wirtszelle, welche in ihr produzierte Viren freisetzt. Im Gegensatz dazu wird beim lysogenen Zyklus die virale Erbsubstanz in das Genom der Wirtszelle integriert, der Virus kann dann als so genannter Prophage in der Wirtszelle weiter existieren. Durch Zellteilung der Prokaryoten wird auch der Virus an die Tochterzellen weitergegeben. Durch Änderung äußerer Einflüsse kann auch der lytische Zyklus wieder aktiviert werden, was zur Produktion von Viren und deren Freisetzung führt. Ein wichtiger Parameter des lytischen Zyklus ist die „burst size" (BS), d. h. die Anzahl an Viren, die während der Lysis von einer infizierten Zelle freigesetzt wird. Bei gemischten, mikrobiellen Gemeinschaften, wie sie *in situ* vorkommen, wird die BS durch Elektronenmikroskopie ermittelt (Weinbauer, 2004). Ein höherer Anteil an Prophagen (Prozentsatz an Prokaryoten, die ein induzierbares, virales Genom enthalten) wird mit niedriger Wirtsabundanz- und aktivität in Verbindung gebracht (Weinbauer et al., 2003; Paul, 2008). Viren können auch genetisches Material zwischen Prokaryoten transferieren, wodurch kurzfristige Anpassungen an wechselnde Umgebungsbedingungen ermöglicht werden könnten (Fuhrman, 1999). Viren können sich nicht bewegen, daher ist virale Infektion ein stochastischer Prozess (Wommack und Colwell, 2000; Weinbauer, 2004), welcher von zahlreichen Faktoren abhängt, wie z. B. Abundanz und Größe der Wirtszellen (Murray und Jackson, 1992). Darüber hinaus sind die meisten Viren wahrscheinlich wirtsspezifisch (Ackermann und DuBow, 1987), nur ein geringer Teil infiziert ein breites Spektrum an Wirten (Riemann und Middelboe, 2002; Weinbauer, 2004). Da statistisch gesehen ein guter Teil aller Prokaryoten permanent infiziert ist, ist es keine Überraschung, dass spezifische Viren-Wirtssysteme eng gekoppelt sind und oftmals Räuber-Beute-Beziehungen zeigen (Gavin et al., 2006; Winter et al., 2010).

Diversität von Viren und Prokaryoten

Viren sind genetisch gesehen die vielfältigste biologische Einheit unseres Planeten, es gibt kein einziges Gen, dass alle bekannten Viren aufweisen (Suttle, 2005). Dieses Fehlen von gemeinsamen Genen in Proben von gemischten Gemeinschaften macht es unmöglich, phylogenetische Beziehungen basierend auf genetischen Daten zu rekonstruieren. Die moderne Systematik von Viren basiert auf der Art von Nukleinsäure (ein- oder doppelsträngige DNA bzw. RNA) und morphologischen Merkmalen wie z. B. filamentöse Form, polyhedrale Form, An- bzw. Abwesenheit eines Schaftes etc. (Ackermann, 2003).

Zahlreiche Experimente zeigten, dass Viren die Gemeinschaften von Prokaryoten beeinflussen (Hewson et al., 2003; Schwalbach et al., 2004; Winter et al., 2004b). Generell wird virale Infektion als top-down Kontrolle prokaryotischer Diversität angesehen im Gegensatz zu einer bottom-up Kontrolle durch anorganische Nährstoffe (z. B. Nitrat, Phosphat) und DOC. Man nimmt an, dass Viren einen hohen Grad an Diversität von Prokaryoten aufrechterhalten, indem sie die häufigsten Typen innerhalb eines bestimmten Zeitintervalls infizieren und damit Prokaryoten mit geringerer Abundanz erlauben wettbewerbsfähig zu bleiben. Obwohl diese so genannte "Killing the winner"-Hypothese (Thingstad und Lignell, 1997; Thingstad, 2000; Winter et al., 2010) auf gleichbleibenden Bedingungen basiert sowie auf der Annahme beruht, dass Viren strikt wirtsspezifisch sind, bietet sie ein leicht verständliches Modell, welches von zahlreichen Arbeiten unterstützt wird (Winter et al., 2010).

Ein großer Beitrag zum gegenwärtigen Wissen über die Ökologie mariner Viren stammt von Inkubationsexperimenten sowie von Untersuchungen kultivierbarer Viren/Wirtssysteme (Wommack und Colwell, 2000; Weinbauer, 2004). Die rasante Entwicklung kulturunabhängiger Methoden in den letzten Jahrzehnten bietet detailliertere Einsicht in die eigentlichen *in situ*-Prozesse. Da der Aufwand, Viren aufgrund ihrer Größe zu untersuchen sowie Proben aus der Tiefsee zu nehmen, sehr hoch ist, gibt es noch viele unbeantwortete Fragen bezüglich der *in situ*-Verhältnisse in der Tiefsee.

Tiefenstufen im subtropischen Atlantik

Das Epipelagial ist die oberste Wasserschicht, sie reicht von der Oberfläche bis zu 200 m Tiefe. Besonders in den oberen 100 m, der euphotischen Zone, gibt es reichlich Sonnenlicht. Vor allem dort findet man das Phytoplankton, photosynthetisch aktive Organismen, die das Sonnenlicht nutzen, um Biomasse aufzubauen. Das Phytoplankton stirbt schließlich ab und sinkt in tiefere Wasserschichten.

Im Mesopelagial, welches von 200 m bis 1000 m Tiefe reicht, ist immer noch schwaches Sonnenlicht vorhanden, man nennt es daher auch „Dimlight zone“. Bei einer Tiefe von 500–700 m misst man im Allgemeinen die niedrigsten Sauerstoff-Konzentrationen eines vertikalen Profils aufgrund von heterotrophen Mikroorganismen, welche die sinkenden Überreste des Phytoplankton remineralisieren. Diese Zone wird daher oxygen minimum zone (OMZ) genannt. Das Bathypelagial ist ein umfangreicher Wasserkörper, es reicht von 1000 m bis 4000 m Tiefe. Da hier kein Licht mehr vorkommt, kann keine Photosynthese mehr stattfinden. Im Bathypelagial vorkommende Mikroorganismen konsumieren absinkendes, organisches Material. Das Abyssopelagial (4000 m Tiefe bis zum Meeresgrund) ist die tiefste in dieser Arbeit behandelte Wassermasse. Der Wasserdruck ist hoch und die Temperaturen sind niedrig, was für die dort lebenden Organismen konstante Bedingungen bedeutet.

Charakteristika und Wassermassen des östlichen, subtropischen Atlantik

Der östliche, subtropische Atlantik hat einen relativ hohen Sauerstoff- und Salzgehalt verglichen mit anderen Meeren (Tomczak und Godfrey, 2001). Teilweise handelt es sich um eine oligotrophe Umgebung, da die Corioliskraft riesige Wirbel (engl. „gyres“) in Form isolierter Wassermassen bildet, was wiederum zu wenig Eintrag von Nährstoffen führt (Ott, 1988). Die Probestationen 2–4 sind näher an der Küste (Figure 3; „onshore“), die restlichen (Stationen 5–8) sind „offshore“ und liegen innerhalb des subtropischen Gyre-Systems. Die verschiedenen Wassermassen des Atlantik können aufgrund von Salinität, Temperatur und Sauerstoffgehalt unterschieden werden. Im nördlichen Atlantik wird das sauerstoffreiche North Atlantic Deep Water (NADW) gebildet, welches sich südwärts entlang des amerikanischen Kontinents bewegt (Tomczak und Godfrey, 2001). Das Antarctic Bottom Water (AABW), das fast den ganzen Grund des Atlantik bedeckt, ist charakterisiert durch niedrige Temperaturen und Salinität sowie durch hohe Silikat- und Nährstoffkonzentrationen (Demidov et al., 2007).

Die Vema Fracture Zone (VFZ) ist ein Riss im Mittelatlantischen Rücken auf einer Tiefe von 5000 m bei Position 11 ° Nord, und 45 bis 40 ° West (Demidov et al., 2007) (Figure 3). Aufgrund dieses 8–20 km breiten Risses ist die Längsachse des Mittelatlantischen Rücken um ca. 300 km versetzt, wodurch der Austausch von Wassermassen zwischen westlichem und östlichem atlantischen Becken ermöglicht wird. Der untere Teil des NADW sowie das kalte und schwere AABW (Table 2) werden durch die VFZ mit Geschwindigkeiten von bis zu 30 cms^{-1} in das östliche Becken des Atlantik bewegt (Demidov et al., 2007). Man nimmt an, dass dieser Fluss an

Wassermassen von West nach Ost mikrobielle sowie virale Gemeinschaften im nordöstlichen, subtropischen Atlantik durch veränderte Nährstoff- und Sauerstoffbedingungen beeinflussen.

Um herauszufinden, ob virale und prokaryotische Gemeinschaften durch den Wassermassenaustausch beeinflusst werden, wurden im Rahmen der MOCA-Cruise im October 2010 Proben aus bis zu 5200 m Tiefe genommen und wichtige Parameter der vorkommenden Prokaryoten und Viren charakterisiert. Im Zuge dieser Diplomarbeit wurden Proben von den ersten 7 Stationen der MOCA-Cruise (Stationen 2–8, Table 1, Figure 3) mit Flow Cytometry und molekularbiologischen Methoden analysiert.

Virenverdünnungsmethode

Bei der Virenverdünnungsmethode werden Prokaryoten mit filtriertem Probenwasser verdünnt und dadurch bei geringerer Dichte inkubiert als bei *in situ*-Verhältnissen (Wilhelm, 2002). Viren, die von bereits infizierten Prokaryoten produziert und freigesetzt werden, können demnach kaum weitere Prokaryoten infizieren, da die Begegnungsrate stark reduziert ist. Aus diesem Grund beruht die gemessene virale Abundanz (Figure 5) auf Viren, die bereits zu Beginn der Inkubation Prokaryoten infiziert hatten und durch deren Lysis freigesetzt wurden. Basierend auf der gemessenen Abundanz in 4 Stunden-Abständen (Figure 5) kann der Prozentsatz an infizierten Prokaryoten (frequency of infected cells = FIC) sowie die im Durchschnitt durch Lysis freigesetzten Viren pro ml pro Stunde (lytic viral production = VP) berechnet werden.

Mitomycin C ist eine Substanz, die Lysis bei infizierten Prokaryoten bewirkt (Jiang und Paul, 1996), d. h., Prophagen im Wirtsgenom wechseln vom lysogenen in den lytischen Zyklus und werden dadurch freigesetzt. Dadurch tragen diese Viren zur gemessenen viralen Abundanz bei. Da das Experiment mit 2 verschiedenen Treatments durchgeführt wurde (mit und ohne Mitomycin C, beides in Duplikaten) kann man den Prozentsatz an lysogenen Viren (frequency of lysogenized cells = FLC) berechnen. Die FLC ist der Unterschied zwischen den Prozent infizierter Prokaryoten im Treatment mit Mitomycin C (enthält nach Induktion sowohl lysogene als auch lytische Viren) und der FIC berechnet aus dem Treatment ohne Mitomycin C (enthält nur lytische Viren).

Zusammensetzung prokaryotischer und viraler Gemeinschaften

Um DNA-fingerprints von *Archaea* und *Bacteria* der verschiedenen Wassermassen zu erhalten, wurde terminal restriction fragment length polymorphism (T-RFLP) (Liu et al., 1997; Moeseneder et al., 1999) durchgeführt (Figure 6). Bei dieser Methode werden Unterschiede in den Längen von 16S rRNA PCR-Fragmenten von *Archaea* und *Bacteria*, die mit einem Restriktionsenzym geschnitten wurden, verglichen. Unterschiede in den Längen reflektieren phylogenetische Unterschiede, ausgedrückt in apparent richness (AR), der Anzahl verschiedener Taxa sowie An- bzw. Abwesenheit der jeweiligen Gruppen in den samples.

Randomly amplified polymorphic DNA-PCR (RAPD-PCR) (Williams et al., 1990; Franklin et al., 1999; Winget und Wommack, 2008) mit 2 unterschiedlichen Oligomer-Primern wurde durchgeführt, um die Viren in den Proben miteinander zu vergleichen. Wie bereits weiter oben erwähnt, sind Viren genetisch gesehen sehr divers. Um das Problem zu umgehen, dass keine gemeinsamen Nukleinsäure-Sequenzen aller Viren existieren und es damit keine allgemeinen Primer wie bei der Amplifizierung von 16S rRNA-Genen gibt, werden bei RAPD-PCR kurze Primer verwendet. Dies führt bei der PCR zu unterschiedlich großen DNA-Fragmenten unabhängig von der exakten Sequenz (Figure 8a).

INTRODUCTION

The role of microorganisms and viruses in the Oceans

The occurrence of relatively high numbers of prokaryotes in the oceans was already known in the first half of the 20th century (Waksman and Renn, 1934; ZoBell, 1946), even though those numbers were underestimated by ca. 3 orders of magnitude since those counts relied on cultivation of the microbes. This deviation of counts from the actual abundance results from the fact, that most prokaryotes are uncultivable (Hugenholtz, 2002) and is therefore called "Great plate count anomaly" (Staley and Konopka, 1985). Until the 1970s, prokaryotes were viewed as terminal decomposers of the food chain with no major contribution to biogeochemical cycling. This view changed in the 1980s. The term "microbial loop" was coined by Azam et al. (1983) and refers to the ability of prokaryotes to take up dissolved organic carbon (DOC) and therefore to form the basis of the food chain, being grazed upon by ciliates and flagellates (Figure 1). Since this DOC derives largely from organisms being part of this food chain, the term "loop" describes the cycling of DOC within this chain (Figure 1). There are several sources of DOC in the oceans such as exudates of phytoplankton, sinking and degraded/degrading planktonic organisms, excretion, sloppy feeding of zooplankton and – important for this thesis – viral lysis (Dafner and Wangersky, 2002).

The earliest findings, that viral infection can be high in prokaryotes and therefore plays an important role in aquatic systems, were made in the late 1980s (Sieburth et al., 1988; Bergh et al., 1989; Proctor and Fuhrman, 1990). The influence of viruses on the mortality of prokaryotes was confirmed, when a similar prokaryotic mortality caused by viruses and protists was discovered (Fuhrman and Noble, 1995). Today it is clear, that mortality of prokaryotes caused by viruses has a great impact on the cycling of organic carbon in aquatic systems (Wommack and Colwell, 2000; Suttle, 2005 and 2007). One difference, however is, that viruses lyse, but do not eat the prokaryotes (despite their name "bacteriophages"), leading to conversion of prokaryotes into non-living DOC available again for other prokaryotes, a circle known as "viral shunt" (Figure 2) (Wilhelm and Suttle, 1999; Suttle, 2005). For that reason, an estimated 20 % of the prokaryotes statistically never contribute to higher trophic levels since they are lysed by viruses before they can be grazed by protists (Wommack and Colwell, 2000).

Some characteristics of viruses

Viruses are the most abundant biological entities in the ocean with an estimated total number of 10^{29} (Suttle, 2007). Despite their small size (size range: 20–400 nm, La Scola et al., 2003), if stringed one after each other, the viruses in the oceans of the world would reach a length of 10 million light years (Suttle, 2005; Suttle, 2007). Viruses are capable of several different "survival" strategies, the most common of which are the lytic and the lysogenic cycle (Weinbauer, 2004; Suttle, 2007). The lytic cycle leads to lysis of the host cell and the viral progeny are subsequently released. In contrast, during the lysogenic cycle, the viral nucleic acid is integrated into the host genome, leading to a "prophage". The virus can remain in the prophage state, leading to the transmission of the viral genome to the host daughter cells, or the lytic cycle can be induced again leading to the production and eventually the release of viruses. In the lytic cycle, the burst size (BS) is an important parameter. The BS is the number of viruses released per infected prokaryotic cell during lysis and, for mixed prokaryotic communities, is usually determined by electron microscopy (Weinbauer, 2004). A higher occurrence of prophages (percentage of prokaryotic cells containing an inducible viral genome; Weinbauer, 2004) is considered to be based on bad environmental conditions in terms of low host abundance and activity (Weinbauer et al., 2003; Paul, 2008). Viruses can also transfer genetic material between prokaryotes, which could influence short term adaptation of prokaryotes to changing environmental conditions (Fuhrman, 1999). Viruses are not capable of movement, therefore infection is a stochastic process (Wommack and Colwell, 2000; Weinbauer, 2004) and it depends on several factors such as host density and size of the hosts (Murray and Jackson, 1992). Moreover, most viruses are assumed to be host specific (Ackermann and DuBow, 1987), only a minority of viruses have a broad host range (Riemann and Middelboe, 2002; Weinbauer, 2004). Since a large part of prokaryotes is infected by viruses at any given time (Wommack and Colwell, 2000) it is not surprising, that specific virus-host systems are closely coupled often displaying predator-prey oscillations (Gavin et al., 2006; Winter et al., 2010).

Diversity of viruses and prokaryotes

Since there is no single gene shared by all viruses, they are considered to be the most genetically diverse biological entities on our planet (Suttle, 2005). The lack of common genes among all viruses in mixed community samples makes it impossible to reconstruct phylogenetic relationships based on molecular data. So far, systematics of viruses is based on the type of nucleic acid (single or double

stranded DNA or RNA) and morphological properties such as presence of a tail, polyhedral shape, filamentous shape etc. (Ackermann, 2003). Several experimental studies showed that viruses influence prokaryotic community composition (Hewson et al., 2003; Schwalbach et al., 2004; Winter et al., 2004b). Viral infection is viewed as a top-down control for prokaryotic diversity, whereas inorganic nutrients such as nitrate and phosphate as well as DOC act as bottom-up controlling agents. It is argued, that viruses maintain a high level of prokaryotic diversity by infecting the most abundant populations over a specific time-course, therefore allowing prokaryotes with lower abundance to compete. Although this "Killing the winner"-hypothesis (Thingstad and Lignell, 1997; Thingstad, 2000; Winter et al., 2010) is based on steady state conditions and on the assumption, that viruses are strictly host specific, it provides a model, which is easy to grasp and which is supported by several studies (reviewed by Winter et al., 2010).

A great deal of recent knowledge of marine viral ecology is derived from incubation experiments and from cultivable phage-host-systems (Wommack and Colwell, 2000; Weinbauer, 2004), but the progressive development of culture-independent methods in the last decades provides more insight into the actual *in situ*-processes. Nevertheless, considering the difficulties in investigating viruses owing to their physical size, and the high effort necessary to take samples from the deep sea, unsolved questions remain due to the difficulty of gathering reliable data of the *in situ*-conditions in deep oceanic waters.

Depth layers in the eastern, subtropical Atlantic

The epipelagic is the layer from the water surface to 200 m depth. Sunlight is found there, especially in the upper 100 m, which is called the euphotic layer. Photosynthetic organisms conducting primary production, the phytoplankton, is found there. This phytoplankton degrades and sinks to deeper water layers. In the mesopelagic, which spans from 200 m to 1000 m depth, weak light still occurs, therefore it is also called "dimlight zone". In the mesopelagic, at a depth of around 500–700 m, the oxygen minimum zone (OMZ) occurs. Oxygen reaches its lowest concentration there, due to microorganisms, which respire sinking organic matter derived from photosynthetic production in the epipelagic. The bathypelagic is a large water mass, it ranges from 1000 m to 4000 m depth. No photosynthesis occurs due to a lack of light. Microorganisms living there consume sinking organic matter. The abyssopelagic is the deepest water layer found in the present study ranging from 4000 m to the bottom. Pressure is high and temperature is low, providing constant conditions for organisms living there.

Characteristics and water masses of the eastern, subtropical Atlantic

The eastern, subtropical Atlantic is characterized by a high oxygen content and a higher salinity compared to the other oceans (Tomczak and Godfrey, 2001). It is partly an oligotrophic environment, since formation of gyres due to the coriolis force leads to isolation of water masses and therefore less input of nutrients (Ott, 1988). Some of the sampling stations (Figure 3) are closer to shore ("onshore", stations 2–4), others (stations 5–8) are offshore and within the subtropical gyre-system. Water masses of the Atlantic can be distinguished by their salinity, temperature, and oxygen-concentration. North Atlantic Deep Water (NADW) is formed in the northern Atlantic and moves, rich in oxygen, southward along the American continent (Tomczak and Godfrey, 2001). Antarctic Bottom Water (AABW) occupies the bottom of almost the whole Atlantic, moves northward west of the Mid-Atlantic Ridge and is characterized by low temperature and salinity, but high silicate and inorganic nutrient concentrations (Demidov et al., 2007).

The Vema Fracture Zone (VFZ) is a crack in the Mid-Atlantic Ridge at a depth of 5000 m at 11 ° North, causing an offset of the ridge of ca. 300 km from 45 to 40 ° West (Demidov et al., 2007) (Figure 3). This fracture with a width of ca. 8–20 km allows the exchange of water masses between the western and the eastern Atlantic basin. The lower part of NADW as well as the cold and dense AABW (Table 2) are pushed through the fracture zone and enter the eastern basin, reaching velocities of up to 30 cms^{-1} (Demidov et al., 2007). The movement of deep water masses from west to east is considered to influence microbial and viral communities found in the northeastern, subtropical Atlantic due to different concentrations of oxygen and nutrients. To find out, whether viruses and their prokaryotic hosts are being influenced, samples during the MOCA-Cruise in October 2010 were taken at depths down to 5200 m and parameters revealing characteristics of viruses and prokaryotes were determined. For this thesis, samples from the first 7 stations of this cruise (stations 2–8, Table 1, Figure 3) were analyzed with flow cytometry and molecular biology methods.

Virus dilution approach

The idea of the dilution technique (Figure 4) is to incubate prokaryotes with greatly reduced abundances than is found *in situ* (Wilhelm, 2002). Prokaryotes already infected by viruses produce and release viruses. Since prokaryotic abundance is low, a strongly reduced encounter rate of viruses and prokaryotes is the result. An increase in viral abundance over the period of incubation (Figure 5)

is therefore a result of viral lysis of the prokaryotes already infected at the beginning of the incubation rather than new infection of the prokaryotes by the released viruses. By this, the percentage of infected prokaryotes (frequency of infected cells = FIC) and the number of viruses released by lysis per ml per hour (lytic viral production = VP) can be calculated based on the abundance determined in 4 hour-intervals (Figure 5).

Mitomycin C acts as an inducing agent, i. e. a substance, which forces prophages in the host genome to switch to the lytic cycle (Jiang and Paul, 1996). These viruses are eventually released and contribute to viral abundance measured in the incubation experiment. Since the experiment was conducted in duplicates of 2 different treatments (with and without Mitomycin C), it is therefore possible to calculate the percentage of lysogenic viruses (frequency of lysogenized cells = FLC). The FLC is the difference between the percentage of infected prokaryotes of treatments with Mitomycin C (which after induction contains both lysogenic and lytic viruses) and FIC of treatments without Mitomycin C (contains only lytic viruses).

Prokaryotic and viral community composition

In order to fingerprint *Archaea* and *Bacteria* found in the sampled water masses, terminal restriction fragment length polymorphism (T-RFLP) (Liu et al., 1997; Moeseneder et al., 1999) was used (Figure 6). This method analyzes differences in the lengths of PCR-amplified fragments of the 16S rRNA gene of *Archaea* and *Bacteria* in a sample cut by a restriction enzyme as an indication of phylogenetic differences between samples. Diversity of prokaryotes and their community composition is in this method reflected in terms of apparent richness (AR) which is the number of occurring taxa as well as presence or absence of those taxa in specific samples.

Randomly amplified polymorphic DNA-PCR (RAPD-PCR) (Williams et al., 1990; Franklin et al., 1999; Winget and Wommack, 2008) using two different oligomer-primers was carried out to fingerprint the viral communities found at each of the 6 depths at each station (Figure 7). As mentioned above, viruses are genetically very diverse. To circumvent the fact, that for amplification by PCR no specific primers as for amplification of 16S rRNA genes in prokaryotes can be used, short “random”-primers lead to differently-sized DNA-fragments independent of their exact sequence (Figure 8a).

MATERIAL AND METHODS

Study area and sampling

All samples were provided by Simone Muck and Christian Winter, who participated in the MOCA-Cruise in October 2010 aboard R/V Pelagia. For this thesis, I got the samples of 7 stations covered during the cruise (Table 1, Figure 3). Water samples identified based on their specific characteristics of temperature, salinity and oxygen (Table 2) were collected at 6 depths from the epi- to the abyssopelagic layer (100–5200 m depth) (Table 2) using a CTD (conductivity-temperature-depth) rosette sampler equipped with 20 l Niskin-bottles.

Prokaryotic and viral abundance

Two ml of samples were fixed with glutaraldehyde (5 % final concentration) for 15 minutes at room temperature, subsequently shock-frozen in liquid nitrogen, and stored at -80 °C until analysis. Prokaryotic and viral abundance was measured as described by Marie et al. (1999) and Brussaard (2004). In short: For enumeration of prokaryotes, samples were thawed at room temperature, diluted with TE-buffer, consisting of MilliQ-water, 10 mM Tris (Tris(hydroxymethyl)-aminomethan), 1 mM EDTA (Ethylenediaminetetraacetic acid), pH 8.0, stained with SYBRGreen I® (Invitrogen, Cat. Nr.: VXS7563) and incubated in the dark for 10 minutes. The prokaryotes were counted on a FACSAria II flow cytometer (Becton Dickinson) by their signature in a plot of SYBR Green I® fluorescence versus side scatter (Figure 9). Particles in TE-buffer and in SYBRGreen I® were considered by measuring and subtracting blanks before calculating abundance values. For enumerating viruses, the procedure was the same, except for incubating the samples in the dark at 80 °C for 10 minutes. The viral abundance was also determined by their signature in a plot of green fluorescence versus side scatter (Figure 9). Based on the same plot, 3 different prokaryotic populations (high nucleic acid, high side scatter = HNAHS, high nucleic acid, low side scatter = HNALS and low nucleic acid = LNA prokaryotes) were distinguished. For viruses, also three different populations were distinguished: high fluorescence (Vir HIGH), medium fluorescence (Vir MED) and low fluorescence (Vir LOW) (Figure 9).

Virus dilution approach to estimate FIC and VP

The Virus dilution-experiment (Figure 4) was carried out at three selected depths per station (meso-, bathy- and abyssopelagic) following the protocol of Wilhelm et al. (2002). Briefly, virus-free water obtained by Tangential-Flow Filtration through spiral-wound ultrafiltration catridges (Amicon S10Y100, 100 kDa molecular weight cut-off) was used to dilute the prokaryotic concentrate obtained by 0.2 µm Tangential Flow Filtration (Pelicon filter-cassettes, PTGVPPC05, 0.22 µm pore-size). The experiments were carried out in duplicates at *in situ* temperatures in the dark, with and without the addition of Mitomycin C (final concentration 1 µg ml^{-1}, Sigma). Mitomycin C was added to induce the lytic cycle of lysogenic viruses. The subsamples for the enumeration of viruses and prokaryotes were taken every 4 h over a period of 32 h. The enumeration (Figure 5) was performed using flow cytometry as described above. FIC, FLC and VP were calculated as described by Winter et al. (2004a) according to the following formulas:

$$\text{Frequency of infected cells (FIC)} = \frac{V_{max1} - V_{min1}}{\text{Burst size} \times P_0} \times 100 \quad (1)$$

$$\text{Frequency of lysogenized cells (FLC)} = FIC_{induced} - FIC \quad (2)$$

$$\text{Lytic viral production (VP)} = \frac{(V_{max1} - V_{min1}) + (V_{max2} - V_{min2}) + (V_{max3} - V_{min3})}{t_{max3} - t_{min1}} \quad (3)$$

When more peaks of viral abundance occurred in the time course of the experiment (Figure 5), the FIC was calculated separately for each peak and these values were added. Values for burst size were not determined in this study, it was assumed to be 30 throughout all of the samples. Calculation of FLC (2) could logically only have been performed, when the mean of FIC of the duplicate treatments including Mitomycin C (induced) was higher than the mean of the 2 treatments without Mitomycin C. Moreover, the calculation was only carried out, when the range of the duplicate treatments with Mitomycin C did not overlap with the range of the 2 treatments without Mitomycin C (control). The formula for calculating viral production (3) is shown for 3 peaks of viral lysis events according to Figure 5.

Prokaryotic community composition

Sampling

Eighteen liters of sample were filtered using the Vivaflow system (Vivaflow 200) in combination with Pelicon filter-cassettes (PTGVPPC05, 0.22 µm pore-size) to concentrate prokaryotes. This prokaryote concentrate was subsequently filtered on 0.2 µm filters with a diameter of 47 mm (Millipore, type GVWP) and those filters were stored at -80 °C.

Extraction of prokaryotic DNA

Prokaryotic DNA for T-RFLP was extracted from the filters using an UltraClean® Soil DNA Isolation Kit (MoBio Laboratories, Inc., Solana Beach, California, Cat. Nr.: 312800-100) according to the manufacturer's instructions and following the alternative lysis protocol to keep shearing of nucleic acids at a low level. Filters were cut with ethanol-flamed scissors and transferred to extraction tubes with ethanol-flamed forceps. Tubes were shaken by hand instead of being vortexed. Extracted DNA, dissolved in 50 µl of buffer S5, was checked on a 1 % agarose (Eurogentec, Molecular biology grade, Cat. Nr.: EP-0010-05) gel (run at 75 V for 120 minutes) for quality. The agarose was dissolved in TBE-buffer (1.34 mol l^{-1} TRIS, 0.44 mol l^{-1} Boric Acid, 0.025 mol l^{-1} EDTA disodium salt dihydrate, pH adjusted to 8.3). The gel was post-stained for 30 min with 0.5 x SYBR® Gold diluted in a TBE-buffer-bath taken from a 10 000 x concentrate (Invitrogen, Cat. Nr.: S11494). DNA-extracts were stored at -80 °C.

Amplification of prokaryotic DNA

Amplification of fragments of the 16S rRNA genes from prokaryotic DNA was performed via PCR using the primers 27F (5'-AGAGTTTGATCCTGGCTCAG-3') and 1492R (5'-GGTTACCTTGTTA CGACTT-3') for *Bacteria* (Lane, 1991) as well as 21F (5'-TTCCGGTTGATCCYGCCGGA-3') and 958R (5'-YCCGGCGTTGAMTCCAATT-3') for *Archaea* (DeLong, 1992). Both forward primers were fluorescently 5′ end-labeled with phosphoramidite fluorochrome 5-carboxy-fluorescein (5′6-FAM), the reverse primers were labeled with VIC (Perkin-Elmer Life Sciences Pty Ltd). Each PCR-reaction included 5 µl of 10x Taq-buffer with KCl (100 mM Tris-HCl with pH 8.8 at 25 °C, 500 mM KCl, 0.8 % Nonidet P40), 4 µl of $MgCl_2$ (25 mM), 1.25 µl of dNTPs (10 mM each), 2.5 µl of each forward and reverse primer (10 µM each) and 0.25 µl of recombinant Taq-Polymerase (5 U $µl^{-1}$) as well as 1 µl of prokaryotic template DNA. All primers, as well as the Taq-Polymerase with supplied buffers (Cat. Nr.: EP0621) were purchased from Thermo-Scientific. Each run included a negative control to check for DNA contamination. Used deoxyribonucleotide triphosphates (dNTPs) were

from Invitrogen (100 mM each, Art. Nr.: dATP: 10216-018, dCTP: 10217016, dGTP: 10218014, dTTP: 10219-012), diluted to 10 mM each. A Mastercycler pro (Eppendorf, Hamburg, Germany) was used for the amplification reaction with the following protocol: Initial denaturation and enzyme activation at 95 °C for 5 min followed by 30 cycles of 95 °C for 1 min (denaturation), 55 °C for 1 min (annealing), and 72 °C for 1 min (extension), with a final elongation step of 30 min at 72 °C to eliminate artifacts (Janse et al., 2004). PCR products were checked by agarose gel electrophoresis (1 %, run at 70 V for 50 minutes) and subsequently purified with a 5Prime PCR Extract MiniKit (Ref. Nr.: 2300610) following the manufacturer's protocol. Prokaryotic 16S rRNA was eluted in 50 µl of buffer PEB of the extraction kit. The concentration of PCR products was measured with a Nanodrop® spectrophotometer.

T-RFLP digest

The purified PCR products were used for the enzyme reaction with *Hha* I (New England Biolabs® Inc., Cat. Nr.: R0139S). A Mastercycler pro (Eppendorf, Hamburg, Germany) was used with the following protocol: Enzyme digestion at 37 °C for 12 hours followed by enzyme deactivation at 65 °C for 20 min and a final hold at 4 °C. Each 15 µl digestion reaction contained 8–10 µl of purified PCR-product, 0.5 µl of restriction enzyme (Hha I, 20 U/µl, Ref. nr.: R0139S), 1.5 µl of 10x NEBuffer 4 (Ref. nr.: B7004S), 0.15 µl of 100x BSA (Ref. nr.: B9001S) and 2.85 µl of H_2O.

Analysis of fragments by capillary electrophoresis

The fluorescently labeled and digested PCR fragments were analyzed by capillary electrophoresis. For each reaction, 10 µl of Hi-Di™ formamide (highly deionized formamide for capillary electrophoresis, Applied Biosystems, Cat. Nr.: 4311320), 0.25 µl Genescan™ 1200LIZ® (Cat. Nr.: 4379950) size marker as well as 1 µl of the T-RFLP digestion reaction were transferred into 96-well microtiter plates, briefly centrifuged, denaturated at 95 °C for 3 min, and subsequently put on ice immediately. Analysis of the fragments was performed using a 3130XL Sequencer (Applied Biosystems) with capillary lengths of 50 cm and running POP-7 polymer.

Data obtained from the sequencer were analyzed using Peak Scanner™ 1.0 Software (Applied Biosystems) considering fragments with a size of 20–1200 bp, For distinguishing signal from noise, an arbitrarily determined peak threshold-height of 30 was chosen and applied to all samples. After analyses and check of the peaks, the data was assembled into a matrix, where the peaks have been aligned based on fragment size. This resulted in four presence/absence matrices (forward and reverse primers for both *Archaea* and *Bacteria*) (Example: Figure 14), which were used for further statistical analysis.

Viral community composition

Samples

The rest of the water after removing and filtering prokaryotes for prokaryotic community samples was filtered through spiral-wound ultrafiltration catridges (Amicon S10Y100, 100 kDa cutoff) to obtain viral concentrates, ca. 30–50 ml of which was then transferred to 50 ml-tubes and stored at -80 °C.

Preparation of viral samples

After thawing the concentrate, it was filtered through 0.2 µm Acrodisc® Syringe Filters (Pall Corporation, Part Nr.: 4192) in order to ensure, that no prokaryotes remained in the samples. Concentration of the samples was performed by ultrafiltration at 4 °C using Amicon® Ultra-15 Centrifugal filter devices (Millipore, Cat. Nr.: UFC910024) with a molecular weight cut-off of 100 kDa. The centrifuge used was an Eppendorf 5810R at 3220 relative centrifugal force. The amount of resulting viral concentrate for further processing was ca. 180 µl.

Extraction of viral DNA

Extraction of viral DNA was performed with QIAamp® MinElute® Virus Spin Kit (Qiagen, Cat. Nr.: 57704). QIAGEN Protease was dissolved in Buffer AVE, 100 µl of the viral concentrate were diluted with 125 µl of 0.9 % (w/v) NaCl solution and then processed according to the protocol of the manufacturer. Extracted viral DNA was eluted in 50 µl AVE buffer and stored at -80 °C.

PCR reactions

For the PCR reactions, two primers were used: OPA-13 (5'-CAGCACCCAC-3') and CRA-22 (5'-CC GCAGCCAA-3') (Wommack et al., 1999) both purchased from Thermo Scientific. Only one of the 2 primers were used in each reaction, acting as both forward and reverse primer (Figure 8). For each run, negative controls were also included, to check for potential DNA contamination of PCR chemicals. Each 50 µl-reaction contained 5 µl of 10x Taq-buffer with KCl (200 mM Tris-HCl pH 8.4, 500 mM KCl), 1.5 µl of 50 mM $MgCl_2$, 1 µl of dNTPs (10 mM each), 5 µl (CRA-22) or 10 µl (OPA-13) of primers, 0.25 µl of Platinum Taq (5 $U\,\mu l^{-1}$) and 5 µl (CRA-22) or 4 µl (OPA-13) of viral template DNA. Taq-Polymerase was Invitrogen Platinum Taq (Cat. Nr.: 10966-018), including 10x Taq-buffer and 50 mM MgCl. Used dNTPs were the same as for amplifying prokaryotic DNA.
The protocol on the cycler (Eppendorf Mastercycler pro) started with initial denaturation and enzyme activation at 94 °C for 10 min, followed by 30 thermal cycles of 94 °C for 30 sec (denaturation),

35 °C for 3 min (annealing) and 72 °C for 1 min (extension) with a final elongation step of 30 min at 72 °C. For reactions containing the primer OPA-13 it was necessary to double the primer volume to obtain good quality bands.

Analysis of the bands by gel electrophoresis

For analysis of the bands, gel electrophoresis using 2.5 % agarose gels in 1xTBE-buffer was performed at 44 V for 135 minutes. The gels were post-stained with SYBR® Gold as described above, pictures of the gels with high resolution were made using a Gel Doc EQ (Bio-Rad) gel documentation system. Analysis of the gels was performed using Quantity One 4.6.8 with a Gel Doc XR+ Plugin. Based on the DNA rulers SmartLadder (Eurogentec, 200–10 000 bp, Ref. Nr.: MW-1700-10) as well as Fermentas gene ruler (250–10 000 bp, Cat. Nr.: SM0311), the occurring bands in the samples were sized. This information was then exported to Microsoft Excel, where an alignment was created. Appearance of specific bands resulted in presence/absence-matrices (Figure 14) for all samples.

Other parameters measured on the ship

Temperature, salinity, and oxygen were measured with sensors on the CTD-device. Prokaryotic heterotrophic production (PHP) was determined as prokaryotic leucine incorporation (in µmol leucine $m^{-3}d^{-1}$) as described by Reinthaler et al. (2006), except that a Tri-carb liquid scintillation counter (PerkinElmer) was used. Measurements of inorganic nutrients were performed according to the Joint Global Ocean Flux study (JGOFS, 1994).

Statistical analysis

Except stated otherwise, statistical analysis was performed using SPSS software (version 15.0.1, SPSS Inc.).

Comparison of different depth layers

For comparing the different parameters with respect to sampling depth, the vertical water mass was separated into four depth layers (Table 2): epipelagic (0–200 m), mesopelagic (200–1000 m), bathypelagic (1000–4000 m) and abyssopelagic (4000–5200 m). Parameters of all seven stations were then summarized and grouped within these layers (Table 4). Since the bathypelagic is a vast water body spanning 3000 m in depth, separate graphs and correlation matrices were made for the lower NADW to check for relations between the parameters. The data were checked if they fit the normal distribution by a Kolmogorow-Smirnov-Test. In case the particular parameter was normally distributed, ANOVA in combination with least square differences (LSD) post-hoc test was performed to compare the depth layers. Kruskal-Wallis one-way analysis of variance on ranked data in combination with Mann-Whitney posthoc and Bonferroni correction using PAST 2.10 (Hammer et al., 2001) was computed for non-normally distributed variables such as prokaryotic and viral abundance.

Comparison of onshore and offshore stations

Since some parameters changed over geographic distance (Figure 5, 6 and 7), the stations were grouped in "onshore" (stations 2–5 for epipelagic, stations 2–4 for bathy- and abyssopelagic) as well as "offshore" (stations 6–8 for epipelagic, stations 5–8 for bathy- and abyssopelagic). Those two groups were then compared using *t*-tests, when the specific parameter was normally distributed (e.g., AR) or using Manny-Whitney-tests, when the parameter was not normally distributed (e.g., prokaryotic abundance).

Correlations

Since the whole dataset of variables measured during the cruise (temperature, salinity, inorganic nutrients, DOC, etc.) was also available, correlations between those variables and the parameters determined in this thesis were also checked. Spearman rank correlation coefficients for all variables against each other were calculated to find related parameters over all depths and separately for each depth layer (Table 5 and 6) as well as specifically for the lower NADW.

In order to calculate the distances between the stations based on the GPS-coordinates shown in Table 1, an online calculator (http://www.gpsvisualizer.com/calculators), which considers the spheroid shape of the Earth was fed with the coordinates of the 7 stations. Geographic distance is expressed as distance in kilometers from station 8 (Figure 5, 6 and 7).

Mantel tests

For comparing prokaryotic and viral community composition with each other or with other parameters, Mantel tests (Mantel, 1967) were calculated from distance matrices using PAST 2.10 (Hammer et al., 2001). Significance of each calculation was determined by 5000 iterations. The calculations were performed on the entire data set as well as on each depth layer alone (as well as for the LNADW only) to pinpoint differences in the specific depth layers controlling prokaryotic and viral communities (Table 7 and 8). Jaccard distance matrices were calculated from the presence/absence matrices obtained by T-RFLP and RAPD-PCR, Bray Curtis-distance matrices were computed from numeric variables such as depth or temperature to be able to compare these parameters to each other. Distance matrices were also calculated from the geographic distances in km between the stations to detect changes of community composition over a geographic scale.

Bonferroni-correction

The results of statistical tests were considered to be significant at p-values < 0.05, except for Bonferroni-correction: Spearman rank-correlations, ANOVA, Kruskal-Wallis-tests and Mantel statistics were corrected using the Bonferroni-Method. This correction was necessary for two reasons: First, stochastic relationships introduced by the co-occurrence of many factors were ruled out, since significance is more likely to occur, when many variables are considered simultaneously (Abdi, 2007). Without correction, this can lead to a wrong impression of significant results. Table 3 shows the grouped parameters and the corrected p-values for each group.

RESULTS

Differences between depth layers

Abundance of viruses and prokaryotes

When data of all stations was combined and average values were calculated, a clear trend of decrease of viral and prokaryotic abundance with depth was visible (Table 4 and 5, Figure 10a). The abundance of prokaryotes decreased by one order of magnitude from 1.6×10^5 (SD = 0.3) in the epipelagic to 0.1×10^5 (SD < 0.1) in the abyssopelagic both being negatively correlated to depth ($r = 0.93$, Table 5). Prokaryotic abundance in the 4 depth layers differed significantly from each other (Kruskal-Wallis: $H = 33.55$, $p \leq 0.001$; Mann-Whitney: all p-values ≤ 0.001) except when comparing bathy- to abyssopelagic (Mann-Whitney: $U = 31$, $p = 0.230$).

Viral abundance was on average ca. 25 times higher than prokaryotic abundance (Table 4), it decreased from the epipelagic (5.0×10^6 ml^{-1}, SD = 1.9) by one order of magnitude towards the bathypelagic (0.417×10^6 ml^{-1}, SD = 0.2), but increased again in the abyssopelagic (0.519×10^6 ml^{-1}, SD < 0.1) (Table 4, Figure 10a). Viral abundance in the epipelagic was significantly different from the meso-, bathy- and abyssopelagic (Kruskal-Wallis: $H = 24.25$, $p \leq 0.001$; Mann-Whitney: all p-values ≤ 0.01). Moreover, the mesopelagic differed significantly from the bathypelagic (Mann-Whitney: $p = 0.005$).

The VP-ratio was high in the epipelagic (30.9, SD = 8.5), lower in the mesopelagic (13.3, SD = 3.3) and high again in the bathy- and abyssopelagic (27.6, SD = 12.7 and 29.2, SD = 9.5, respectively) (Table 4, Figure 10a). VP in the mesopelagic differed significantly from the epi-, bathy- and abyssopelagic (Kruskal-Wallis: $H = 20.58$, $p \leq 0.001$; Mann-Whitney: all p-values ≤ 0.010).

Prokaryotic and viral populations

The percentage of HNALS-prokaryotes was significantly lower in the epipelagic than in the other depth layers (Kruskal-Wallis: $H = 15.95$, $p = 0.001$; Mann-Whitney: all p-values < 0.010), no difference was found between meso-, bathy- and abyssopelagic (Figure 10c). HNAHS-prokaryotes were found to be significantly lower in the mesopelagic compared to all other depth layers (Kruskal-Wallis: $H = 28.72$, $p \leq 0.001$; Mann-Whitney, all p-values ≤ 0.001) (Figure 10c). A significant difference was also found when comparing bathy- to abyssopelagic (Mann-Whitney: $p \leq 0.001$), with HNAHS being higher in the abyssopelagic. The percentage of LNA-prokaryotes decreased almost

linear with depth (Table 4, Figure 10c), with significant differences between some of the depth layers (Kruskal-Wallis: $H = 24.34$, $p \leq 0.001$).

The average in the epipelagic differed significantly from bathy-, and abyssopelagic (Mann-Whitney: p-values ≤ 0.003) and the percentage in the mesopelagic was significantly higher than in bathy-, and abyssopelagic (Mann-Whitney: p-values ≤ 0.003). Percentage of LNA-prokaryotes in the bathypelagic differed also significantly from the abyssopelagic (Mann-Whitney: $p = 0.004$).

Vir LOW did not show any significant trend over depth, neither did Vir MED (Figure 10c), the latter of which constituted the most abundant group of viruses in all depth layers (Table 4). The percentage of Vir HIGH was significantly higher in the epipelagic from all other depth layers (Kruskal-Wallis: $H = 15.78$, $p = 0.001$; Mann-Whitney, all p-values ≤ 0.005).

FIC and VP

FIC increased significantly with depth ($r = 0.74$, Table 5, Figure 10b) from 23.1 % in the mesopelagic, over 27.7 % in the bathypelagic to 57.0 % in the abyssopelagic. FIC in the abyssopelagic was significantly different from the values determined in meso- and bathypelagic (Kruskal-Wallis: $H = 9.55$, $p = 0.008$; Mann-Whitney: all p-values ≤ 0.01).

VP decreased rapidly from 38.5×10^3 $ml^{-1} h^{-1}$ in the mesopelagic to 7.9×10^3 $ml^{-1} h^{-1}$ in the bathypelagic and differed significantly between the two depth layers (Kruskal-Wallis: $H = 11.94$, $p = 0.003$; Mann-Whitney: $p = 0.002$). In the abyssopelagic, VP increased again (10.56×10^3 $ml^{-1} h^{-1}$), although not significant. No significant correlation between VP and depth was found.

AR of prokaryotes and number of RAPD-PCR bands of viruses

Although AR of *Bacteria* decreased significantly with depth (*Bacteria* reverse, $r = -0.42$, Table 5) (Table 4, Figure 10d), no statistically significant difference was found between the four depth layers (one-way ANOVA: *Bacteria* forward: $F = 0.87$, $p = 0.467$; *Bacteria* reverse: $F = 1.71$, $p = 0.184$). Bacterial AR (forward primer) was related to depth in the abyssopelagic only ($r = 0.94$, Table 5). AR of *Archaea* and the number of viral bands did not show any significant change over depth (one-way ANOVA: *Archaea* forward: $F = 1.10$, $p = 0.365$; *Archaea* reverse: $F = 2.07$, $p = 0.123$; CRA: $F = 2.36$, $p = 0.081$; OPA: $F = 0.99$, $p = 0.412$).

Differences over geographic distance

Epipelagic

When considering the epipelagic only, viral abundance decreased from 6.3×10^6 ml^{-1} at station 2 to 3.6×10^6 ml^{-1} at station 8 (Figure 11a). Prokaryotic abundance was more or less constant over geographic distance (1.578×10^5 ml^{-1} at station 2, 1.452×10^5 ml^{-1} at station 8) (Figure 11a), for that reason, VP-ratio showed a similar trend as virus abundance and decreased from 40.1 to 24.0 (Figure 11a). When grouping Stations 2–5 (onshore) and Stations 6–8 (offshore) and comparing the means of the 2 groups by a *t*-test, a significant difference was observed for viral abundance ($t = 7.89$, $p \leq 0.001$) and also for VP-Ratio ($t = 7.07$, $p \leq 0.001$). Temperature also decreased from Station 2 to 8 (Figure 11b), and significantly correlated with geographic distance ($r = 0.89$, Table 5). Nitrate (NO_3), phosphate (PO_4) and silicate (SiO_4) significantly increased towards station 8 in the epipelagic (Table 6).

Mesopelagic and bathypelagic

In the mesopelagic, only nitrate ($r = -0.95$) and phosphate ($r = 0.92$) were significantly correlated to geographic distance (Table 6): nitrate increased and phosphate decreased towards station 8. In the bathypelagic, FIC and oxygen increased, nitrate and phosphate decreased from station 2 to 8 (Table 6).

When examining the lower part of the NADW (7 samples taken at 2969–3397 m depth, Table 2), an increase of both VP and FIC towards station 8 was visible (Figure 12a and b). VP increased by a factor of ca. 2 from 4.42×10^3 ml^{-1} h^{-1} at station 2 to 9.51×10^3 ml^{-1} h^{-1} at station 8. FIC increased by a factor of 2.6 from 13.9 % at station 2 to 36.8 % at station 8. AR of *Bacteria* determined by the forward primer increased almost 7-fold from station 2 to station 8 (Figure 12f).

Other parameters that changed with geographic distance were temperature, oxygen, nitrate and phosphate. Oxygen increased almost linear (Figure 12d) with significant correlation to geographic distance ($r = -0.96$, $p \leq 0.001$). Temperature, nitrate and phosphate decreased significantly towards station 8 (all *r*-values ≥ 0.89, all *p*-values ≤ 0.007). When comparing onshore and offshore-stations by *t*-test or Mann-Whitney-test, significant differences were found for the following parameters: FIC ($t = -3.07$, $p = 0.037$), salinity ($t = 2.64$, $p = 0.046$), oxygen ($t = -0.39$, $p = 0.012$), phosphate ($t = 3.59$, $p = 0.016$) and AR *Bacteria* forward ($t = -5.05$, $p = 0.004$). No significant change of viral or prokaryotic abundance over geographic distance was observed in the LNADW.

Abyssopelagic

In the AABW, VP was significantly higher when comparing means of the onshore stations against the offshore-stations ($t = 7.0$, $p = 0.002$) (Figure 13b). The temperature dropped from 2.39 °C at station 3 to 2.18 °C at station 8 and was correlated to geographic distance ($r = 0.94$, $p = 0.005$) (Figure 13b). When comparing means of the temperature at the stations onshore to the stations offshore by *t*-test, a significant difference was found ($t = 3.16$, $p = 0.034$). Nitrate increased significantly with decreasing geographic distance to station 8 ($r = -0.94$, $p = 0.005$) (Figure 13d). Silicate-concentrations at stations offshore were significantly higher than onshore ($t = -4.99$, $p = 0.008$). Prokaryotic and viral abundance did not show any significant trend over geographic distance in the abyssopelagic, neither did the VP-Ratio.

Other relationships between parameters

Abiotic factors, oxygen, inorganic nutrients, DOC and PHP

Correlations of the parameters with abiotic factors are depicted in Table 5, relationships to each other or to other parameters such as PHP, oxygen and nutrient concentrations are shown in Table 6 and briefly summarized here: Prokaryotic abundance was correlated to viral abundance ($r = 0.72$), FIC ($r = -0.73$), VP ($r = 0.44$), PHP ($r = 0.95$), oxygen ($r = -0.76$) and SiO_4 ($r = -0.90$), viral abundance to all of the parameters, except VP. These relationships were found over the whole data set as well as in the mesopelagic. The VP-Ratio was over all depths strongly correlated to oxygen ($r = 0.62$), both decreased from epi- to the mesopelagic and increased again in the deeper layers. FIC was negatively correlated to viral abundance ($r = -0.57$) and to PHP ($r = -0.62$), but increased with oxygen and silicate. Furthermore, VP vorrelated with PHP ($r = 0.53$) and nitrate ($r = 0.58$). The VP-ratio was correlated to FIC ($r = 0.56$) and VP ($r = -0.50$) in the entire data set, as well as to oxygen, nitrate and phosphate.

The concentration of dissolved organic carbon (DOC) was significantly correlated to FIC in the whole dataset ($r = 0.56$), increased with geographic distance in the bathypelagic ($r = -0.85$) and was negatively correlated with the VP-ratio in the abyssopelagic ($r = -0.94$) (DOC-data not shown).

Prokaryotic and viral populations

Viral abundance correlated positively with LNA-prokaryotes ($r = 0.52$), but negatively with HNALS-prokaryotes ($r = -0.46$). In the whole dataset, HNAHS-prokaryotes were connected to FIC ($r = 0.75$), oxygen ($r = 0.75$) and inorganic nutrients (nitrate: $r = -0.61$; phosphate: $r = -0.59$). In the mesopelagic,

HNAHS was positively correlated with oxygen ($r = 0.67$) and VP in the bathypelagic ($r = 0.74$). Overall, FIC and oxygen decreased with increasing LNA-prokaryotes ($r = -0.73$ and -0.76). Also, the higher PHP, the more LNA-prokaryotes were found ($r = 0.76$). Vir HIGH was correlated to prokaryotic abundance ($r = 0.65$) and also to PHP over all depths ($r = 0.68$) and in the bathypelagic ($r = 0.76$ and 0.59). Vir LOW and Vir MED appeared to play a role in the abyssopelagic, where they were positively ($r = 0.94$) and negatively ($r = -0.94$), correlated to PHP, respectively (Table 6).

AR of *Archaea* and *Bacteria* and number of viral RAPD-PCR bands

The forward primer of *Bacteria* yielded DNA fragments with a size ranging from 21–1132 bp (in total 92 peaks). Two most abundant peaks occurred at 33 and 902 bp, both being present in 41 of 42 samples (97.6 %). For the reverse primer, the smallest fragment measured 24 bp and the longest 930 bp, resulting in a total of 73 peaks. The 133 bp-fragment appeared in all of the 42 samples, 16 fragments were only detected once. In contrast, analysis of the archaeal forward primer resulted in a total of 18 different DNA-fragments with sizes of 26–912 bp. The 321 bp-fragment was present in all of the samples, 11 other fragments were present only one time in one single sample. The archaeal reverse primer resulted in 18 different fragments with a size range from 28 to 933 bp with the most abundant one appearing in all samples having a size of 585 bp. Six fragments were present only one time in one sample. AR of *Archaea* reverse was on average significantly higher than *Archaea* forward ($t = 4.1$, $p = 0.004$), no significant difference was found between AR of the bacterial primers.

The size of viral RAPD-PCR products ranged from 196–2918 bp for the CRA-primer, with 2 most abundant bands at 596 bp and 1615 bp, both being present in 90.5 % of the samples. Bands with the size of 196 bp, 215 bp, and 2918 bp were only present in 1 sample (2.4 %) (Figure 14). Band-sizes of the OPA-primer ranged from 212–3671 bp, the most abundant band had a size of 983 bp, being present in 73.8 % of the samples. Only 1 band (212 bp) was present in one sample (2.4 %).

Community composition of prokaryotes and viruses

Relationships between prokaryotic and viral community composition

Using mantel tests, relations between the community composition of forward- and reverse-primers of *Archaea* and *Bacteria*, respectively were found in the entire data set ($r_M = 0.47$ for *Archaea*, $r_M = 0.77$ for *Bacteria)* as well as in most depth layers (Table 7): Forward and reverse primers of *Bacteria*

were connected in all depth layers (r_M ranging from 0.64–0.80), forward and reverse primers of *Archaea* were only connected in the mesopelagic ($r_M = 0.63$) and bathypelagic ($r_M = 0.43$). A connection between CRA- and OPA-primers was only found in the mesopelagic ($r_M = 0.38$). When the community composition of prokaryotes with the one of viruses was compared, relationships were found only between *Bacteria* forward and CRA (bathypelagic, $r_M = 0.24$) and *Bacteria* forward and OPA (abyssopelagic, $r_M = 0.38$).

Influence of other parameters on prokaryotic and viral communities

Table 8 shows the relationship of abiotic and biotic parameters with the community composition of prokaryotes and viruses. For the entire data set, depth, temperature and salinity influenced archaeal, bacterial and viral communities stronger (r_M ranging from 0.13–0.37) than geographic distance (r_M ranging from 0.11–0.18). There was also a relationship between prokaryotic abundance and prokaryotic and viral communities (r_M ranging from 0.18–0.39). Viral abundance was related to archaeal community composition (forward primer: $r_M = 0.29$), bacterial community composition (forward primer: $r_M = 0.39$, reverse primer: $r_M = 0.29$), and viral community composition (CRA, $r_M = 0.34$). PHP seemed to play an important role, and was related to archaeal community composition (forward primer: $r_M = 0.23$), bacterial communities (forward primer: $r_M = 0.38$; reverse primer: $r_M = 0.33$) and viral community composition (CRA, $r_M = 0.33$). Nitrate, nitrite and phosphate were related to bacterial community composition (r_M ranging from 0.27–0.34) and CRA (r_M ranging from 0.30–0.32). Silicate was also related to bacterial (r_M ranging from 0.18–0.34) as well as viral (CRA, $r_M = 0.25$) community composition, oxygen-concentration only showed a weak connection to OPA ($r_M = 0.18$). Ammonia was related to viral community composition in the meso- (CRA, $r_M = 0.43$) and bathypelagic (OPA, $r_M = 0.38$). Viral communities changed over geographic distance in the mesopelagic (CRA, $r_M = 0.30$) and bacterial communities changed in the bathypelagic with geographic distance ($r_M = 0.18$ and 0.28).

When considering the LNADW only (data not shown), both oxygen and geographic distance were significantly related to bacterial community composition. Geographic distance was linked to bacterial community composition ($r_M = 0.52$ and 0.65 for forward and reverse, respectively; p for both ≤ 0.01), and oxygen ($r_M = 0.45$ and 0.77, respectively; p for both ≤ 0.01). VP in the LNADW was connected to the community composition of *Archaea* (forward primer: $r_M = 0.44$, $p = 0.027$), prokaryotic abundance was related to viral community composition (CRA: $r_M = 0.50$, $p = 0.018$).

In the abyssopelagic, depth, salinity and VP were related to bacterial community composition (r_M ranging from 0.66 to 0.71). Viral community composition (OPA) was connected to VP ($r_M = 0.82$) and phosphate ($r_M = 0.54$).

DISCUSSION

Critical evaluation of the techniques

Virus dilution approach

Advantages and disadvantages of the dilution approach were reviewed by Winget et al. (2005) and are briefly summarized here: Advantages include the simple and inexpensive equipment needed as well as the chance to observe changes of viral abundance over the time of incubation (Figure 5). Disadvantages are a slight influence on the prokaryotic communities in the sample while performing Tangential Flow Filtration and the high amount of sub-samples needed. However, the large amount of counts is not much of a problem when using flow cytometry, which has been shown to be a reliable method since flow cytometry-counts are similar to epifluorescence counts (Brussaard et al., 2010). Decay of viruses was not taken into account in the present study, probably leading to a slight underestimation of FIC and VP especially in the mesopelagic, since viral decay was shown to be one order of magnitude lower in deep waters and depends on temperature (Parada et al., 2009).

T-RFLP

T-RFLP was introduced in 1997 (Liu et al.) as a high throughput method for characterizing the diversity of microorganisms. It has been applied to ribosomal genes and also functional genes of prokaryotes (Schütte et al., 2008). The use of polyacrylamide gels was shown to be not as reproducible and the resolution is lower than using capillary gel electrophoresis for separating differently-sized fragments described by Behr et al. (1999). The accuracy of the analysis by capillary electrophoresis is high (differences of ± 1 bp; Moeseneder et al., 1999; Schütte et al., 2008), although this accuracy decreases with longer DNA-fragments. Comparison of the same samples run several times showed a variability of the size fragments of only ± 1 bp (Schütte et al., 2008), which is in line with the observation of analyzing duplicate or triplicate samples done in the present study (data not shown). Identification of members of microbial communities as described by Schütte et al. (2008) was not considered to be a reliable approach, since one specific fragment could be due to the presence of different prokaryotic phylotypes and not just one.

RAPD-PCR

Compared to other methods such as pulsed field gel electrophoresis (PFGE), the resolution of RAPD-PCR is higher (Winget and Wommack, 2008). However, it is possible that some viral groups cannot be distinguished by agarose gel electrophoresis, limiting the method (Winter and Weinbauer,

2010). Another factor one has to keep in mind is, that only the nucleic acids of DNA-viruses were extracted using the QIAamp® MinElute® Virus Spin Kit. In addition, only viruses with priming sites for the primers could be detected (Figure 8). RAPD-PCR using one specific primer detects only a subset of viruses in the sample, as suggested by Winter and Weinbauer (2010). But since the number of database entries of viral genomes currently is low, this needs further investigation. The potential disadvantage of fingerprinting only a subset of viruses is minimized due to the use of 2 different primers, CRA and OPA, targeting different subsets of the virus community (Winter and Weinbauer, 2010). As described for T-RFLP, determining the relative contribution of the groups is not possible for RAPD-PCR due to PCR-biases (Winter and Weinbauer, 2010).

Nevertheless, other potential drawbacks have been shown to be minimal. For example, since RAPD-PCR was also successfully applied to prokaryotes (Franklin et al., 1999; Winter and Weinbauer, 2010) and eukaryotes (Williams et al., 1990; Winter and Weinbauer, 2010), the question arises, whether the amplified products are of viral origin only. This objection can easily be refused, since the viral template for PCR was viral concentrate (obtained from 18 l sample water) produced by Tangential Flow Filtration, which is a reliable method (Winget et al., 2005) and then additionally filtered through 0.2 µm filters to assure removal of all prokaryotic cells and other organisms. One general problem of PCR is chimera formation (Brakenhoff et al., 1991). Chimeric sequences are artefacts created during PCR. However, studies using RAPD-PCR and viral nucleic acid sequencing did not find any chimeric products at all (Rohwer et al., 2001; Winget and Wommack, 2008). Finally, there are two potential reasons for a wrong estimate of the observed viral diversity in comparison to the actual viral diversity: First, overestimation of viral genetic diversity by more than one priming site for a specific virus resulting in more than one band. Second, underestimation, if genetically different viral strains result in bands of the same size. These possible estimation-errors were shown by Winget and Wommack (2008) not to be a problem. By sequencing the amplified PCR-products after purification, the authors found that “most bands are likely derived from single viral strains within the original assemblage”. Furthermore, no homology between bands from the same profile was found. Despite these drawbacks and the fact that RAPD-PCR will not sample the diversity of the whole viral community, the method is reproducible and reliable (Winget and Wommack, 2008).

Prokaryotic and viral parameters

Abundance and VP-Ratio

Viral abundance with an average of 1.3×10^6 ml^{-1} is typical for marine environments (Wommack and Colwell, 2000; Weinbauer, 2004) and also typically low for oligotrophic open ocean areas. Also the decrease of abundance with depth of both viruses and prokaryotes was as expected and shown in several studies (Wommack and Colwell, 2000; Weinbauer, 2004). The positive correlation of viral and prokaryotic abundance (Table 6) is not surprising, since a higher density of prokaryotes increases the probability for a virus to find a host and therefore increases also the adsorbtion rate (Murray and Jackson, 1992). In addition, more prokaryotes can maintain a higher number of viruses. Viruses also show a higher variability in the measurements compared to prokaryotes (Table 4), confirming that viral abundance is less tightly controlled than abundance of prokaryotes (Weinbauer, 2004).

Compared to a similar study conducted further south in the Atlantic Ocean (De Corte et al., 2010), viral abundance as well as the VP-Ratio were higher in the present study. Viral abundance was almost twice as high, VP-Ratio three times as high in the epipelagic, the differences in deeper water layers are smaller. For prokaryotic abundance, it was the other way around, it was found to be higher in the water samples taken further south. De Corte et al. found an increasing VP-Ratio with depth, which was not the case in the present study (Table 4, Figure 10a). VP-Ratio only differs drastically in the mesopelagic, being less than half found in the other 3 depth layers. However, the Cruise of De Corte et al. (2010) was undertaken at a different time of the year (December 2007/January 2008) than the MOCA-Cruise (October 2010) relevant for the present study. Seasonal variation of prokaryotic and viral parameters was reported by several other authors (Wommack and Colwell, 2000; Winter and Weinbauer, 2010).

Prokaryotic abundance was slightly higher and viral abundance was two- to three times higher in another study in the northeast, subtropical Atlantic (Parada et al., 2007) compared to the present study when considering similar depths. The authors concluded that the high number of viruses found in the meso- and bathypelagic in that study could have been the result of allochthonous input of viruses or high (pseudo)lysogenic production.

The tight coupling of both viral and prokaryotic abundance with PHP found in this study (Table 6) is well known, since more prokaryotes simply incorporate more leucine and more viruses were found to occur in more productive systems (Weinbauer, 2004). Maintenance of a high number of viruses depends on an active prokaryotic host community (Wommack and Colwell, 2000).

Prokaryotic and viral populations

The positive relationship of LNA-prokaryotes to PHP is at first glance unexpected, since other studies (Lebaron et al., 2001) have shown the HNA-fraction of prokaryotes being the main drivers of bulk PHP with values up to 100 % of HNA-prokaryotes to be responsible for the activity determined by leucine incorporation. However, this relationship does not necessarily mean, that all of the HNA-prokaryotes have high cell-specific rates of production, since there was a great variety of activity determined for this group of prokaryotes. The major part of LNA-prokaryotes was in that study considered being mainly inactive or dead. However, one particular sampling site (SOLA 1/SOLA 2) of the study conducted by Lebaron et al. (2001) showed the weakest correlation between HNA-prokaryotes and PHP and the highest incorporation rates of leucine by LNA-prokaryotes. Prokaryotic abundance at that sampling site was of similar magnitude as in the present study, moreover oligotrophic conditions were also found at SOLA. In contrast, there are also studies (Zubkov et al., 2004; Sherr et al., 2006; Talarmin et al., 2011) showing that LNA-prokaryotes are important contributors to PHP. Zubkov et al. (2004) hypothesized that in coastal bacterioplankton communities off Plymouth (UK), LNA-content in prokaryotes is an adaptation to oligotrophic environments. Sherr et al. (2006) found, that HNA-prokaryotes are good predictors for high prokaryotic activity in coastal, productive marine ecosystems with high phytoplanktic biomass. In offshore waters however, both HNA- and LNA-prokaryotes are not as well related to prokaryotic activity with a higher variation of parameters there. In contrast to the study of Lebaron et al. (2001), the authors concluded that the LNA-prokaryotes cannot be considered inactive or dead. The third mentioned study (Talarmin et al., 2011) confirmed that both HNA- and LNA-prokaryotes are important contributors to PHP in the open Mediterranean Sea. These indications could mean that PHP in eutrophic environments like coastal areas is mainly driven by HNA-prokaryotes in contrast to the oligotrophic open ocean, where LNA-prokaryotes constitute the group being responsible for a major part of PHP.

The connection between HNAHS-prokaryotes and FIC (r = 0.75, Table 6) could be an indication, that those prokaryotes are more susceptible to viral infection. In contrast, LNA-prokaryotes do not appear to be infected to such a high extent (correlation with FIC: r = -0.73, Table 6), which could be an additional reason, why PHP can thrive among LNA-prokaryotes, since their activity is not hindered by viral infection.

The finding, that Vir MED-populations were the most abundant ones, was also found by De Corte et al. (2008). These viruses seem to be dominant in pelagic, deep waters, whereas viruses with low fluorescence were found to be dominant in coastal regions (Kimmance et al., 2007; Pan et al., 2007). De Corte et al. (2010) suggested a relation between larger prokaryotic genomes and Vir HIGH in the abyssopelagic, since prokaryotes are assumed to be opportunists there.

HNA-prokaryotes do not correlate with depth in the present study, however, LNA-prokaryotes decrease significantly with depth (Table 5). Vir HIGH shows a decrease with depth to the bathypelagic, with a slight increase in the abyssopelagic (Table 4, Figure 10). This trend is similar to the one found by De Corte et al. (2010).

FIC and VP

Critical for the calculation of FIC is the BS as depicted in Formula (1). As summarized by Parada et al. (2006), the parameters controlling BS are numerous (diversity, size and morphology of hosts and viruses, physiology, productive state of the environment, diel cycles etc.). However, a relation of BS in mixed communities and PHP based on average data for different environments was discovered in the same study. In contrast, in a study conducted by Weinbauer et al. (2003), BS did not change significantly over depth in the Mediterranean Sea. Since BS was not specifically assessed in the present study and the factors controlling BS seem to be too complex to extrapolate values from other environments, the BS was assumed to be 30 over the whole depth range which is a sensible estimate according to Wommack and Colwell (2000) and Parada et al. (2006).

The occurrence of a low FIC in the epipelagic, where prokaryotic and viral abundance was high, is counterintuitive, but shows, that higher viral abundance does not automatically lead to a higher infection rate. The increase in FIC with depth could be related to the occurrence of fewer predators in deeper waters and therefore more viral infection. A higher FIC could result in a higher release of inorganic nutrients and DOC by lysis of prokaryotes. FIC is negatively correlated to PHP, which was also found by Winter et al. (2004). The more cells infected, the lower their production, which makes sense, since viruses could influence activity of their hosts (Weinbauer, 2004). Increase of VP with depth as well as values comparable to the ones in the present study were also found by De Corte et al. (2010). VP, intuitively, should be positively linked to prokaryotic abundance and PHP (Table 6), since more active cells can maintain and produce more viruses. A depth-related trend can be ruled out, since percentages of those viral populations were stable in the 3 depth layers, where also VP was determined. The inverse relationship between VP and VP-ratio when considering the FIC also is somehow a paradox: More viruses per prokaryotic cell should lead to an increased infection rate and also to an increased production of viruses, assuming steady state-conditions. But since FIC was lower in the mesopelagic, more viruses have to be released per lytic event, to maintain the comparatively high number of viruses. In the mesopelagic, only a small fraction of prokaryotes is infected, but produces a high number of viruses. It is the other way around in the abyssopelagic. This suggests, that the factors controlling viral parameters are different in deep waters at the sampling site, or, as mentioned above, the used BS estimate is not constant, but rather changes with depth.

Lysogeny

Since calculation of FLC was possible for only 3 samples, they were excluded from further statistical analyses. One explanation for the low occurrence of lysogeny could be that Mitomycin C did not work as inducing agent for all prokaryotic groups as shown elsewhere (Ackermann and DuBow, 1987). Another possibility however is, that there simply are very few lysogens in the investigated stations and depth layers. Jiang and Paul (1998) found a higher FLC in isolates from offshore, oligotrophic environments and suggested that lysogens only contribute significantly to viral production during natural induction events. Steward and Levin (1984) formulated a hypothesis, after which lysogeny is the dominant survival strategy at low host abundance. Weinbauer et al. (2003) discovered average values of lysogeny 6 times higher in the deep waters compared to surface waters of the Mediterranean Sea. FLC increased toward less productive environments, whereas FIC increased toward more productive environments. The authors therefore suggested that either viral lysis or lysogeny predominates in different environments, depending on the conditions (especially productivity) and that lysogeny is favored under disadvantageous environmental conditions. The Mediterranean Sea is known to be a phosphate-limited environment, with a Redfield-ratio (ratio of N:P, Redfield et al., 1963) between 19–23 in contrast to a typical Redfield-ratio of 16 for other marine systems (Karafistan et al., 2002). Since other studies (Wilson et al., 1998) found lysogeny being prevalent under nutrient (especially phosphorous) limited conditions, this substance among others may play a specific role, if either the lytic or lysogenic cycle dominates (Wilson et al., 1997). Evidence for that also comes from investigations of freshwater environments (Lymer and Lindström, 2010; Pradeep Ram and Sime-Ngando, 2010). Lymer and Lindström (2010) found, that phosphate even induced prophages and resulted in subsequent production of temperate phages. Although host abundance is low in the present study (Table 4, Figure 10), other factors seem to be responsible for the occurrence of only few lysogens. Due to more or less stable concentrations of phosphorous in the water column (Table 4), phosphorous does not seem to be limiting in the northeast, subtropical Atlantic. This could be the main reason, why so few lysogens were found even at greater depths and why lysis is the dominant strategy of prokaryotic viruses at the sampled stations.

Community composition and AR of prokaryotes

The composition of prokaryotic communities seems to be influenced stronger by depth than by geographic distance. Mantel tests have shown positive connections of prokaryotic community composition to depth, but only for *Bacteria* reverse and CRA, in contrast to geographic distance (Table 8). Vertical structuring of marine prokaryotes and viruses was shown in several other studies (reviewed by Wommack and Colwell, 2000; Weinbauer, 2004). However, seasonal mixing of

different depth layers was also reported in deep waters of the Mediterranean Sea (Winter et al., 2009).

A relation of prokaryotic community composition to inorganic nutrients is also evident. Nutrients such as nitrate and phosphate influence prokaryotes by bottom up-control with different phylotypes being adapted in different ways. Influence of inorganic nutrients on viral communities (CRA-primer, Table 8) is indirect and probably a result of a change of prokaryotic communities.

The connection between HNALS-prokaryotes and bacterial community composition might indicate, that those populations are mainly responsible for the bulk structure of bacterial types. The percentage of HNALS-prokaryotes is only significantly different in the epipelagic, supporting this idea, since covariation with depth does not seem to play a role.

A change in FIC was not related to a change in community composition of prokaryotes as reported by Winter et al. (2008). Bacterial AR is almost the same for both primers, with no significant difference. Higher average values with a lower range were found by Winter et al. (2008) in the subtropical Atlantic off the African coast. However, the deepest sampling spot was 1000 m in that study, whereas the lowest values of bacterial AR were found in the bathypelagic in the present study. According to Winter et al. (2008), bacterial AR of the forward primer was higher than the AR given by the reverse primer.

No trend of bacterial AR over depth was found by Winter et al. (2009). However, the study of De Corte et al. (2010) revealed a twofold increase in bacterial AR from 2750 m to >5000 m depth. The authors therefore suggested a wider host range of viruses in deep waters compared to surface waters. The method used in that study was automated ribosomal intergenic spacer analysis (ARISA), targeting the intergenic spacer-region in the rRNA operon. A direct comparison of the values to the ones obtained by T-RFLP is not possible, but comparing relative values of different depth layers within one method should be possible. Archaeal AR was low compared to bacterial AR (Table 4). Values for the archaeal reverse primer were significantly higher than for the archaeal forward primer (Table 4), which was also found in the study of Winter et al. (2008). The values in the present study are lower, but comparable with the values found by De Corte et al. (2010).

Since prokaryotic community composition changed with depth (Table 8), but AR did not (Table 4), a potential shift of the communities with a more or less constant number of different types can be assumed. The same holds true for community composition and number of bands of viruses (Table 4 and Table 8).

Community composition and number of bands of viruses

As for prokaryotes, viral communities differ also with respect to their depth (Table 8). A higher number of bands for CRA than for OPA was also found by Winter and Weinbauer (2010). Since the PCR for OPA did not work in my study (or showed only very weak bands) with the initial primer-concentration, an increase of primer-volume from 5 µl to 10 µl in each PCR-reaction resulted in well visible bands. The reason is probably, that using only 5 µl of primers, not all of the priming sites were covered by primers. An amplification product is only formed, when the primers attach to a paired priming site (Figure 8). With a higher amount of primers, enough paired priming sites were covered, leading to sufficient amplification products. The observed communities of *Bacteria* and viruses considered by the methods used, appear to be tighter coupled in the bathy- and abyssopelagic compared to shallower depths, since viral and prokaryotic communities were connected only there (Table 7).

Characteristics and comparison of the specific depth layers

Change of parameters over geographic distance in the epipelagic

A decrease of viral abundance from onshore-to offshore-stations (Figure 11) was found also in the gulf of Mexico (Boehme et al., 1993; Cochlan et al., 1993) and could be the result of higher productivity closer to the shore. The decrease of viral abundance while prokaryotic abundance did not change in the epipelagic (Figure 11) might be related to bacterial community composition (Table 8). This suggests, that even in the epipelagic, the detected viruses are primarily viruses infecting prokaryotes.

When calculating a regression of *Bacteria* (forward and reverse primer combined), a positive relation with VP-Ratio is the result ($y = 1.25x - 5.81$; $r^2 = 0.96$). The VP-Ratio therefore corresponds to bacterial diversity, the higher the ratio, the higher the diversity. This supports the "Killing the winner"-hypothesis (Thingstad and Lignell, 1997; Thingstad, 2000; Winter et al., 2010), according to which viruses maintain prokaryotic diversity by infecting the most abundant groups.

Influence of deep water masses originating in the western Atlantic basin

In the bathypelagic, where NADW was sampled, FIC as well as oxygen increases towards the VFZ (Table 6, Figure 6). The measured increase of oxygen could be the result of input of oxygen-rich NADW from the western basin, where the flow of NADW occurs southward after being formed in the North-west Atlantic (Ott, 1986; Tomczak and Godfrey, 2002). The input also seems to have some

significant influence on the community composition of *Bacteria*, as data of forward and reverse primers change over geographic distance (Table 8). Changing parameters in the bathypelagic become even more visible, when confining the analysis to samples taken from the lower NADW at around 3000 m depth. Several factors including FIC and VP showed a clear trend over geographic distance, although not statistically significant (Figure 6). One possible reason for the higher FIC towards station 8 could be, that input of viral strains from the western basin could lead to a higher infection of prokaryotes, since those might not be resistant against allochthonous viruses. PHP did not show any trend in the LNADW, although it is correlated to VP over all depths.

In the AABW, VP also increased towards station 8 (Figure 13a). In contrast to the LNADW, FIC did not show any trend. Another difference is the increase of nitrate- and phosphate-concentrations in the AABW closer to station 8 (Figure 13d) in contrast to LNADW, emphasizing that the 2 water masses show distinct characteristics.

Silicate (SiO_4) concentrations were high in AABW. Different concentrations of silicate and the lack of a similar trend over geographic distance in the LNADW and AABW (Figure 12f and 13e) suggest, that the two water masses are clearly separated from each other. Therefore, LNADW and AABW show some distinct patterns of change of specific parameters over geographic distance being probably influenced by input from the western Atlantic basin through the VFZ.

Acknowledgments

I thank my supervisors Christian Winter and Gerhard Herndl. Christian always had an open ear for me and got me interested in marine viral ecology in the first place. Further thank goes to Simone Muck and Adam Klimiuk for conducting the experiments during the cruise and also to Thomas Reinthaler, who provided additional data gathered on the cruise such as nutrients, PHP etc. Christian Baranyi was very helpful in the lab and with explaining some nasty statistics, Daniele De Corte gave precious advice how to interpret the results. I wish also to thank Douglas Adams (“The hitchhiker’s guide to the galaxy”) for supporting my belief, that a sample number of 42 would explain everything in the universe including the relationships between viruses and their prokaryotic hosts in deep waters of the northeastern subtropical Atlantic.

LITERATURE

Abdi, H., 2007: The Bonferroni and Šidák Corrections for Multiple Comparisons. In: Neil Salkind (Ed.), Encyclopedia of Measurement and Statistics. Thousand Oaks (CA).

Ackermann, H.-W., 2003: Bacteriophage observations and evolution. Res. Microbiol. 154, 245–251.

Ackermann, H.W., DuBow, M.S., 1987: Viruses of prokaryotes. In: General properties of Bacteriophages. CRC, Boca Raton, FL, USA, Vol. 1.

Aristegui, J., Gasol, J.M., Duarte, C.M., Herndl, G.J., 2009: Microbial oceanography of the dark ocean's pelagic realm. Limnol. Oceanogr. 54(5), 1501–1529.

Azam, F., Fenchel, T., Field, J.G., Gray, J.S., Meyer-Reil, L.A., Thingstad, F., 1983: The Ecological Role of Water-Column Microbes in the Sea. Mar. Ecol. Prog. Ser. 10, 257–263.

Behr, S., Mätzig, M., Levin, A., Eickhoff, H., Heller, C., 1999: A fully automated multicapillary electrophoresis device for DNA analysis. Electrophoresis 20, 1492–1507.

Bergh, Ø., Børsheim, K.Y., Bratbak, G., Heldal, M., 1989: High abundance of viruses found in aquatic environments. Nature 340, 467–468.

Boehme, J., Frischer, M.E., Jiang, S.C., Kellogg, C.A., Pichard, S., 1993: Viruses, Bacterioplankton, and Phytoplankton in the Southeastern Gulf of Mexico: Distribution and Contribution to Oceanic DNA Pools. Mar. Ecol. Prog. Ser. 97, 1–10.

Brakenhoff, R.H., Schoenmakers, J.G., Lubsen, N.H., 1991: Chimeric cDNA clones: a novel PCR artifact. Nucleic Acids Res. 19(8), 1949.

Brussaard, C.P.D., Marie, D., Bratbak, G., 2000: Flow cytometric detection of viruses. J. Virol. Methods 85, 175–182.

Brussaard, C.P.D., 2004: Optimization of Procedures for Counting viruses by Flow Cytometry. Appl. Environ. Microbiol. 70, 1506–1513.

Brussaard, C.P.D., Payet, J.P., Winter, C., Weinbauer, M.G., 2010: Quantification of aquatic viruses by flow cytometry, p. 102–109. In: Wilhelm, S.W., Weinbauer, M.G., Suttle, C.A. [eds.], Manual of Aquatic Viral Ecology. ASLO.

Cochlan, W.P., Wikner, J., Steward, G.F., Smith, D.C., Azam, F., 1993: Spatial distribution of viruses, bacteria and chlorophyll *a* in neritic, oceanic and estuarine environments. Mar. Ecol. Prog. Ser. 92, 77–87.

Dafner, E.V., Wangersky, P.J., 2002: A brief overview of modern directions in marine DOC studies Part II—Recent progress in marine DOC studies. J. Environ. Monit. 4, 55–69.

De Corte, D., Sintes, E., Winter, C., Yokokawa, T., Reinthaler, T., Herndl, G.J., 2010: Links between viral and prokaryotic communities throughout the water column in the (sub)tropical Atlantic Ocean. ISME J. 4, 1431–1442.

DeLong, E.F., 1992: Archaea in coastal marine environments. Proc. Natl. Acad. Sci. USA 89, 5685–5689.

Demidov, A.N., Dobrolyubov, S.A., Morozov, E.G., Tarakanov, R.Yu., 2007: Transport of Bottom Waters through the Vema Fracture Zone in the Mid-Atlantic Ridge. Doklady Earth Sciences 416, 1120–1124.

Fenchel, T., 2008: The microbial loop – 25 years later. J. Exp. Mar. Biol. Ecol. 366, 99–103.

Fuhrman, J.A., Nobel, R.T., 1995: Viruses and protists cause similar bacterial mortality in coastal seawater. Limnol. Oceanogr. 40(7), 1236–1242.

Fuhrman, J.A., 1999: Marine viruses and their biogeochemical and ecological effects. Nature 399, 541–548.

Franklin, R.B., Taylor, D.R., Mills, A.L., 1999: Characterization of microbial communities using randomly amplified polymorphic DNA (RAPD). J. Microbiol. Methods 35, 225–235.

Gasol, J.M., Zweifel, U.L., Peters, F., Fuhrman, J.A., Hagström, Å., 1999: Significance of size and nucleic acid content heterogeneity as measured by flow cytometry in natural planktonic bacteria. Appl. Environ. Microbiol. 65, 4475–4486.

Gavin, C., Pokrovskii, A., Prentice, M., Sobolev, V., 2006: Dynamics of a Lotka-Volterra type model with applications to marine phage population dynamics. JPCS 55, 80–93.

Hammer, Ø., Harper, D.A.T., Ryan, P.D., 2001: PAST: Paleontological Statistics software package for education and data analysis. Palaeontol. Electron. 4(1), 9 pp.

Hara, S., Koike, I., Terauchi, K., Kamiya, H., Tanoue, E., 1996: Abundance of viruses in deep oceanic waters. Mar. Ecol. Prog. Ser. 145, 269–277.

Hewson, I., Vargo, G.A., Fuhrman, J.A., 2003: Bacterial diversity in shallow oligotrophic marine benthos and overlying waters: effects of virus infection, containment, and nutrient enrichment. Microb. Ecol. 46, 322–336.

Hugenholtz, P., 2002: Exploring prokaryotic diversity in the genomic era. Genome Biology 3(2), reviews 0003.1–0003.8.

Janse, I., Bok, J., Zwart, G., 2004: A simple remedy against artificial double bands in denaturing gradient gel electrophoresis. J. Microb. Methods 57, 279–281.

Jiang, S.C., Paul, J.H., 1996: Occurrence of lysogenic bacteria in marine microbial communities as determined by prophage induction. Mar. Ecol. Prog. Ser. 142, 27–38.

Jiang, S.C., Paul, J.H., 1998: Significance of Lysogeny in the Marine Environment: Studies with Isolates and a Model of Lysogenic Phage Production. Microb. Ecol. 35(3), 235–243.

Kanagawa, T.F., 2003: Bias and artifacts in multitemplate polymerase chain reactions (PCR). J. Biosci. Bioeng. 96(4), 317–323.

Karafistan, A., Martin, J.-M., Rixen, M., Beckers, J.M., 2002: Space and time distributions of phosphate in the Mediterranean Sea. Deep-Sea Research I 49, 67–82.

Kimmance, S.A., Wilson, W.H., Archer, S.D., 2007: Modified dilution technique to estimate viral versus grazing mortality of phytoplankton: limitations associated with method sensitivity in natural waters. Aquat. Microb. Ecol. 49, 207–222.

Lane, D.J., 1991: 16S/23S rRNA sequencing. In: Stackebrandt, E,, Goodfellow, M. (eds): Nucleic acid techniques in bacterial systematics. Wiley, New York, pp 115–176.

La Scola, B., Audic, S., Robert, C., Jungang, L., De Lamballerie, X., Drancourt, M., Birtles, R., Claviere, J.-M., Raoult, D., 2003: A giant Virus in Amoebae. Science, 299(5615), 2033 pp.

Lebaron, P., Servais, P., Agogué, H., Courties, C., Joux, F., 2001: Does the High Nucleic Acid Content of Individual Bacterial Cells Allow Us To Discriminate between Active Cells and Inactive Cells in Aquatic Systems? Appl. Environ. Microbiol. 67, 1775–1782.

Liu, W.T., Marsh, T.L., Cheng, H., Forney, L.J., 1997: Characterization of microbial diversity by determining terminal restriction fragment length polymorphisms of genes encoding 16S rRNA. Appl. Environ. Microbiol. 63, 4516–4522.

Lymer, D., Lindström, E.S., 2010: Changing phosphorus concentration and subsequent prophage induction alter composition of a freshwater viral assemblage. Freshwater Biology 55, 1984–1996.

Mantel, N., 1967: The detection of disease clustering and a generalized regression approach. Cancer Res. 27, 209–220.

Marie, D., Brussaard, C.P.D., Thyrhaug, R., Bratbak, G., Vaulot, D., 1999: Enumeration of marine viruses in culture and natural samples by flow cytometry. Appl. Environ. Microbiol. 65, 45–52.

Moeseneder, M.M., Arrieta, J.M., Muyzer, G., Winter, C., Herndl, G.J., 1999: Optimization of terminal-restriction fragment length polymorphism analysis for complex marine bacterioplankton communities and comparison with denaturing gradient gel electrophoresis. Appl. Environ. Microbiol. 65(8), 3518-3525.

Murray, A.G., Jackson, G.A., 1992: Viral dynamics: a model of the effects of size, shape, motion and abundance of single-celled planktonic organisms and other particles. Mar. Ecol. Prog. Ser. 89, 103–116.

Ott, J., 1988: Meereskunde: Einführung in die Geographie und Biologie der Ozeane. UTB für Wissenschaft, Ulmer, Stuttgart.

Pan, L.A., Zhang, J., Zhang, L.H., 2007: Picophytoplankton, nanophytoplankton, heterotrohpic bacteria and viruses in the Changjiang Estuary and adjacent coastal waters. J. Plankton Res. 29, 187–197.

Parada, V., Herndl, G.J., Weinbauer, M.G., 2006: Viral burst size of heterotrophic prokaryotes in aquatic systems. J. Mar. Biol. Assoc. U.K. 86, 613–621.

Parada, V., Sintes, E., Van Aken, H.M., Weinbauer, M.G., Herndl, G.J., 2007: Viral Abundance, Decay, and Diversity in the Meso- and Bathypelagic Waters of the North Atlantic. Appl. Environ. Microbiol. 73, 4429–4438.

Paul, J.H., 2008: Prophages in marine bacteria: dangerous molecular time bombs or the key to survival in the seas? ISME J. 2, 579–589.

Pradeep Ram, A.S., Sime-Ngando, T., 2010: Resources drive trade-off between viral lifestyles in the plankton: evidence from freshwater microbial microcosms. Environmental Microbiology 12(2), 467–479.

Proctor, L.M., Fuhrman, J.A., 1990: Viral mortality of marine bacteria and cyanobacteria. Nature 343, 60–62.

Redfield, A.C., Ketchum, B.H., Richards, F.A., 1963: The influence of organisms on the composition of sea-water. In: Hill, M.N. (Ed.), The Sea, Vol. 2. Wiley, New York, pp. 26–77.

Reinthaler, T., van Aken, H., Veth, C., Aristegui, J., Robinson, C., Williams, P.J. le B., Lebaron, P., Herndl, G.J., 2006: Prokaryotic respiration and production in the meso- and bathypelagic realm of the eastern and western North Atlantic basin. Limnol. Oceanogr. 51(3), 1262-1273.

Riemann, L., Middelboe, M., 2002: Temporal and spatial stability of bacterial and viral community compositions in Danish coastal waters as depicted by DNA fingerprinting techniques. Aquat. Microb. Ecol. 27, 219–232.

Rohwer, F., Seguritan, V., Choi, D.H., Segall, A.M., Azam, F., 2001: Production of shotgun libraries using random amplification. Biotechniques 31, 108–118.

Schütte, U.M.E., Abdo, Z., Bent, S.J., Shyu, C., Williams, C.J., Pierson, J.D., Forney, L.J., 2008: Advances in the use of terminal restriction fragment length polymorphism (T-RFLP) analysis of 16S rRNA genes to characterize microbial communities. Appl. Microbiol. Biotechnol. 80, 365–380.

Schwalbach, M.S., Hewson, I., Fuhrman, J.A., 2004: Viral effects on bacterial community composition in marine plankton microcosms. Aquat. Microb. Ecol. 34, 117–127.

Sherr, E.B., Sherr, B.F., Longnecker, K., 2006: Distribution of bacterial abundance and cell-specific nucleic acid content in the Northeast Pacific Ocean. Deep-Sea Research I 53, 713–725.

Sieburth, J.M., Johnson, P.W., Hargraves, P.E., 1988: Ultrastructure and ecology of *Aureococcus anophagefferens* gen. et sp. nov. (Chrysophyceae) the dominant picoplankter during a bloom in Narragansett Bay Rhode Island USA summer 1985. J. Phycol. 24, 416–425.

Staley, J.T., Konopka, A., 1985: Measurements of in situ activities of nonphotosynthetic microorganisms in aquatic and terrestrial habitats. Annu. Rev. Microbiol. 39, 321–346.

Steward, G.F., Smith, D.C., Azam, F., 1996: Abundance and production of bacteria and viruses in the Bering and Chukchi seas. Mar. Ecol. Prog. Ser. 131, 287–300.

Suttle, C.A., 2005: Viruses in the sea. Nature 437, 356–361.

Suttle, C.A., 2007: Marine viruses – major players in the global ecosystem. Nat. Rev. Microbiol. 5, 801–812.

Talarmin, A., Van Wambeke, F., Catala, P., Courties, C., Lebaron, P., 2011: Flow cytometric assessment of specific leucine incorporation in the open Mediterranean. Biogeosciences 8, 253–265.

Thingstad, T.F., Lignell, R., 1997: Theoretical models for the control of bacterial growth rate, abundance, diversity and carbon demand. Aquat. Microb. Ecol. 13, 19–27.

Thingstad, T.F., 2000: Elements of a theory for the mechanisms controlling abundance, diversity, and biogeochemical role of lytic bacterial viruses in aquatic systems. Limnol. Oceanogr. 45, 1320–1328.

Tomczak, M., Godfrey, J.S., 2002: Regional Oceanography: An Introduction. 2nd Edition. Daya Publishing House, Delhi.

Tu, O., Knott, T., Marsh, M., Bechtol, K., Harris, D., Barker, D., Bashkin, J., 1998: The influence of fluorescent dye structure on the electrophoretic mobility of end-labeled DNA. Nucleic Acid Res. 26, 2797–2802.

Villarreal, L., 2001: Persisting viruses could play role in driving host evolution. Am. Soc. Microbiol. News 67, 501–507.

Waksman, S., Renn, C., 1934: The role of bacteria in the cycle of life in the sea. Sci. monthly 38, 35–49.

Weinbauer, M.G., Brettar, I., Hofle, M.G., 2003: Lysogeny and virus-induced mortality of bacterioplankton in surface, deep, and anoxic marine waters. Limnol. Oceanogr. 48, 1457–1465.

Weinbauer, M.G., 2004: Ecology of prokaryotic viruses. FEMS Microbiol. Rev. 28, 127-181.

Wilhelm, S.W., Suttle, C.A., 1999: Viruses and nutrient cycles in the sea. Bioscience 49, 781–788.

Wilhelm, S.W., Bridgen, S.M., Suttle, C.A., 2002: A dilution technique for the direct measurement of viral production: a comparison in stratified and tidally mixed coastal waters. Microb. Ecol. 43, 168–173.

Williams, J.G.K., Kubelik, A.R., Livak, K.J., Rafalski, J.A., Tingey, S.V., 1990: DNA polymorphisms amplified by arbitrary primers are useful as genetic markers. Nucleic Acids Res. 18, 6531–6535.

Wilson, W.H., Mann, N.H., 1997: Lysogenic and lytic viral production in marine microbial communities. Aquat. Microb. Ecol. 13, 95–100.

Wilson, W.H., Turner, S., Mann, N.H., 1998: Population Dynamics of Phytoplankton and Viruses in a Phosphate-limited Mesocosm and their Effect on DMSP and DMS Production. Estuar. Coast. Shelf Sci. 46, 49–59.

Winget, D.M., Williamson, K.E., Helton, R.R., Wommack, K.E., 2005: Tangential flow diafiltration: an improved technique for estimation of virioplankton production. Aquat. Microb. Ecol. 41, 221–232.

Winget, D.M., Wommack, K.E., 2008: Randomly Amplified Polymorphic DNA PCR as a Tool for Assessment of Marine Viral Richness. Appl. Environ. Microbiol. 74, 2612–2618.

Winter, C., Herndl, G.J., Weinbauer, M.G., 2004a: Diel cycles in viral infection of bacterioplankton in the North Sea. Aquat. Microb. Ecol. 35, 207–216.

Winter, C., Smit, A., Herndl, G.J., Weinbauer, M.G., 2004b: Impact of virioplankton on archaeal and bacterial community richness as assessed in seawater batch cultures. Appl. Environ. Microbiol. 70, 804–813.

Winter, C., Moeseneder, M.M., Herndl, G.J., Weinbauer, M.G., 2008: Relationship of Geographic Distance, Depth, Temperature, and Viruses with Prokaryotic Communities in the Eastern Tropical Atlantic Ocean. Microb. Ecol. 56, 383–389.

Winter, C., Kerros, M.-E., Weinbauer, M.G., 2009: Seasonal and depth-related dynamics of prokaryotes and viruses in surface and deep waters of the northwestern Mediterranean Sea. Deep-Sea Research I 56, 1972–1982.

Winter, C., Weinbauer, M.G., 2010: Randomly amplified polymorphic DNA reveals tight links between viruses and microbes in the bathypelagic zone of the Northwestern Mediterranean Sea. Appl. Environ. Microbiol. 76, 6724–6732.

Winter, C., Bouvier, T., Weinbauer, M.G., Thingstad, T.F., 2010: Trade-Offs between Competition and Defense Specialists among Unicellular Planktonic Organisms: the "Killing the Winner" Hypothesis Revisited. Microbiol. Mol. Biol. R. 74, 42–57.

Wommack, K.E., Ravel, J., Hill, R.T., Colwell, R.R., 1999: Hybridization analysis of Chesapeake Bay virioplankton. Appl. Environ. Microbiol. 65/1, 241–250.

Wommack, K.E., Colwell, R.R., 2000: Virioplankton: viruses in Aquatic Ecosystems. Microbiol. Mol. Biol. R. 64, 69–114.

ZoBell, C., 1946: A monograph on hydrobacteriology. Chron. Bot. 115.

Zubkov, M.V., Allen, J.I., Fuchs, B.M., 2004: Coexistence of dominant groups in marine bacterioplankton community — a combination of experimental and modelling approaches. J. Mar. Biol. Ass. U.K. 84, 519–529.

APPENDIX

Tables

Table 1 Geographic position, sampling date, deepest sample and bottom depth at the specific stations. Station 1 was a test station and is therefore not part of this study.

Station	Latitude (°N)	Longitude (°W)	Sampling date	Deepest sample (m)	Bottom depth (m)
2	24.45	-20.49	2010-10-11	3902	4023
3	22.17	-23.58	2010-10-12	4700	4930
4	19.91	-26.60	2010-10-13	4399	4703
5	17.81	-29.43	2010-10-14	4502	4638
6	15.86	-32.03	2010-10-15	5198	5465
7	13.64	-34.73	2010-10-16	5198	6107
8	11.38	-37.43	2010-10-17	4998	5241

Table 2 Depth layers, sampled depths, water masses and their characteristics. AABW=Antarctic Bottom Water, AAIW=Antarctic Intermediate Water, BEL=Bottom of euphotic layer, OMZ=Oxygen minimum zone, UNADW, LNADW=upper and lower North Atlantic Deep Water.

Depth layer	Depth	Water mass	Sampled depth	Characteristics
Epipelagic	0–200 m	BEL	100–101 m	light, high temp. and O_2-conc.
Mesopelagic	200–1000 m	OMZ	374–597 m	low O_2-conc.
		AAIW	772–1000 m	low salinity
Bathypelagic	1000–4000 m	UNADW	1976–2081 m	high O_2-conc.
		LNADW	2969–3397 m	high O_2-conc.
Abyssopelagic	4000–5200 m	AABW	4399–5198 m	cold, dense, high silicate

Table 3 Grouped parameters for Bonferroni-correction. The resulting *p*-values were applied to Spearman-correlations (Table 5 and 6) and Mantel-tests (Tab. 7 and 8). DOC=Dissolved organic carbon, FIC=Frequency of infected cells, PHP=Prokaryotic heterotrophic production, VP=Viral production.

Grouped parameters	No. of parameters	corr. p-value
Depth, Temperature, Salinity	3	0.017
Oxygen, DOC, PO_4, NH_4, NO_3, NO_2, SiO_4	7	0.007
Prokaryotic and viral abundance, VP-Ratio, populations	9	0.006
FIC, VP, PHP	3	0.017

Table 4 Mean, standard deviation (SD), range and number of samples of all parameters for the entire data set and for the specific depth layers. AR = apparent richness, DOC = dissolved organic carbon, FIC = frequency of infected cells, fwd = forward, HNALS/HNAHS = high nucleic acid high/low side scatter porkaryotes, LNA = low nucleic acid prokaryotes, PHP = prokaryotic heterotrophic production, rev = reverse, Vir LOW / Vir MED / Vir HIGH = low, medium and high fluorescent viruses, VP-ratio = Virus-to-prokaryote ratio, VP = viral production.

Parameter	Mean (SD)										Range					No. of samples				
	Epi		Meso		Bathy		Abysso		all		Epi	Meso	Bathy	Abysso	all	E	M	B	A	all
Prokaryotes ($\times 10^5$)	1.559	(0.303)	0.582	(0.280)	0.165	(0.061)	0.141	(0.046)	0.523	(0.542)	1.182–2.084	0.309–1.229	0.099–0.321	0.109–0.233	0.10–2.08	7	13	16	6	42
HNALS (%)	28.0	(5.3)	37.2	(4.4)	37.5	(1.9)	37.7	(2.4)	35.8	(4.9)	21.1–34.1	31.8–46.1	33.8–40.6	35.3–41.6	21.1–46.1	7	13	16	6	42
HNAHS (%)	17.4	(5.1)	9.8	(1.8)	15.1	(2.0)	18.8	(1.6)	14.4	(4.2)	12.0–26.6	7.1–13.9	9.5–17.8	16.3–20.7	7.1–26.6	7	13	16	6	42
LNA (%)	54.6	(3.6)	52.7	(4.5)	47.7	(3.1)	43.5	(2.3)	49.8	(5.1)	50.5–60.8	45.9–59.6	43.3–56.3	39.7–45.6	39.7–60.8	7	13	16	6	42
Viruses ($\times 10^6$)	4.950	(1.917)	0.756	(0.353)	0.417	(0.156)	0.519	(0.040)	1.292	(1.829)	2.359–7.018	0.269–1.495	0.097–0.713	0.449–0.559	0.097–7.018	7	13	16	6	42
Vir LOW (%)	31.4	(12.9)	42.7	(20.1)	43.9	(25.9)	31.2	(14.9)	39.6	(21.1)	14.9–54.0	17.9–69.4	18.0–96.4	18.9–57.4	14.9–96.4	7	13	16	6	42
Vir MED (%)	54.6	(13.1)	47.3	(20.1)	47.4	(25.3)	59.4	(15.1)	50.3	(20.7)	31.1–68.8	20.2–73.5	2.7–73.8	33.2–71.7	2.7–73.8	7	13	16	6	42
Vir HIGH (%)	14.1	(2.9)	9.9	(1.7)	8.7	(2.5)	9.3	(0.9)	10.1	(2.8)	10.6–18.7	7.0–13.8	0.8–12.6	8.1–10.8	0.8–18.7	7	13	16	6	42
VP-Ratio	30.9	(8.5)	13.3	(3.3)	27.6	(12.7)	29.2	(9.5)	25.4	(12.8)	20.0–40.1	7.9–18.6	7.1–45.5	24.0–49.5	7.1–49.5	7	13	16	6	42
FIC (%)	-	-	23.1	(7.1)	27.7	(15.0)	57.0	(13.2)	34.0	(18.6)	-	12.7–33.6	6.8–53.7	39.2–67.6	6.8–67.6	-	6	8	5	19
VP ($\times 10^3 ml^{-1} h^{-1}$)	-	-	38.5	(17.8)	7.9	(2.6)	10.6	(2.2)	18.3	(17.1)	-	11.0–63.5	3.3–10.1	7.2–12.6	3.3–63.5	-	6	8	5	19
AR *Bacteria* fwd	18.4	(9.9)	14.7	(6.1)	15.7	(10.0)	11.2	(4.0)	15.2	(8.2)	9–38	6–28	4–32	7–18	4–38	7	13	16	6	42
AR *Bacteria* rev	19.9	(6.2)	15.2	(5.3)	15.4	(8.4)	11.5	(4.0)	15.6	(6.9)	13–30	7–25	3–27	7–18	3–30	7	13	16	6	42
AR *Archaea* fwd	3.3	(1.3)	4.1	(1.1)	3.4	(1.3)	3.2	(1.6)	3.6	(1.3)	1–5	2–6	2–6	2–6	1–6	7	13	16	6	42
AR *Archaea* rev	5.6	(1.3)	6.0	(1.4)	4.4	(2.4)	4.3	(2.4)	5.1	(2.0)	4–7	3–8	1–10	3–9	1–10	7	13	16	6	42
No. of bands CRA	17.6	(3.8)	17.6	(2.9)	20.0	(3.8)	17.7	(3.3)	18.4	(3.5)	10–21	14–25	15–27	14–21	10–27	7	13	16	6	42
No. of bands OPA	16.9	(3.5)	13.6	(4.5)	14.9	(4.8)	13.7	(2.7)	14.7	(4.3)	12–20	7–21	7–21	10–18	7–21	7	13	16	6	42
Temperature (°C)	18.6	(2.5)	8.7	(2.7)	3.5	(1.4)	2.3	(0.07)	7.5	(5.9)	13.8–21.3	5.5–13.7	2.4–7.2	2.2–2.4	2.2–21.3	7	13	16	6	42
Salinity	36.5	(0.5)	35.2	(0.3)	34.9	(0.08)	34.9	(0.01)	35.3	(0.6)	35.5–36.9	34.8–35.9	34.9–35.22	34.9–34.9	34.8–36.9	7	13	16	6	42
Oxygen ($\mu mol kg^{-1}$)	158.7	(36.2)	105.6	(34.3)	214.9	(26.9)	230.9	(2.2)	174.8	(59.6)	116.3–209.8	49.5–157.0	146.4–232.4	228.3–234.5	49.5–234.5	5	13	16	6	40
PHP ($\mu mol\ Leu m^{-3} d^{-1}$)	87.42	(27.21)	1.96	(1.82)	0.09	(0.11)	0.04	(0.01)	15.21	(34.32)	48.49–123.14	0.27–5.18	0.03–0.41	0.03–0.06	0.03–123.14	7	13	16	6	42
NO_3 ($\mu mol kg^{-1}$)	10.70	(8.77)	30.69	(5.44)	23.19	(1.89)	23.71	(0.12)	23.50	(8.10)	0.03–1.65	14.99–36.72	21.25–28.56	23.51–23.83	0.03–36.72	7	13	16	6	42
NH_4 ($\mu mol kg^{-1}$)	0.078	(0.018)	0.064	(0.027)	0.064	(0.021)	0.072	(0.016)	0.068	(0.022)	0.057–0.110	0.036–0.125	0.035–0.102	0.050–0.096	0.035–0.125	7	13	16	6	42
PO_4 ($\mu mol kg^{-1}$)	0.68	(0.52)	1.94	(0.39)	1.56	(0.11)	1.61	(0.01)	1.54	(0.52)	0.03–1.65	0.87–2.27	1.42–1.89	1.60–1.62	0.03–2.27	7	13	16	6	42
SiO_4 ($\mu mol kg^{-1}$)	3.08	(2.58)	17.97	(6.66)	31.92	(9.10)	51.20	(2.24)	25.55	(50.86)	0.53–8.37	5.25–26.71	19.39–48.60	49.04–54.59	0.53–54.59	7	13	16	6	42
DOC ($\mu mol kg^{-1}$)	61.20	(5.98)	48.01	(3.44)	47.38	(4.65)	55.96	(9.80)	50.86	(7.45)	55.69–72.10	42.63–54.22	42.38–56.68	43.46–72.27	42.38–72.27	6	13	16	6	41

Table 5 Spearman rank correlation coefficients (r) for different parameters against depth, temperature and salinity over the whole dataset and in the specific depth layers. All possible combinations were calculated, only significant results are shown here (see also Table 3). Dashes indicate no significant correlation, $0.5 < r < -0.5$ printed in bold. FIC = frequency of infected cells, PHP = prokaryotic heterotrophic production, VP = lytic viral production.

	Depth	Temperature	Salinity	n
All depths				
Prokaryotic abundance	**-0.93**	**0.92**	**0.75**	42
LNA	**-0.78**	**0.76**	**0.57**	42
Viral abundance	**-0.65**	**0.66**	**0.61**	42
Vir HIGH	**-0.58**	**0.59**	**0.52**	42
FIC	**0.74**	-	**-0.74**	19
AR *Bacteria* reverse	-0.42	0.44	-	42
PHP	**-0.92**	**0.92**	**0.77**	42
Epipelagic				
Geographic distance	-	**0.89**	-	7
Mesopelagic				
Prokaryotic abundance	**-0.95**	**0.84**	**0.80**	13
Viral abundance	**-0.86**	-	-	13
Bathypelagic				
Prokaryotic abundance	**-0.71**	**0.65**	**0.64**	16
Abyssopelagic				
HNAHS	-	-	**-0.94**	6
VP	-	-	**-1.00**	5
AR *Bacteria* forward	**0.94**	-	-	6
Geographic distance	-	**0.94**	-	6

Table 6 Spearman rank correlation coefficients (*r*) of determined parameters compared to each other over the whole dataset and in the specific depth layers. All possible combinations were calculated, only significant results are shown here (see also Table 3). Dashes indicate no significant relationship, $0.5 < r < -0.5$ printed in bold. FIC = frequency of infected cells, PHP = prokaryotic heterotrophic production, Prok ab = prokaryotic abundance, Vir ab = viral abundance, VP = lytic viral production, n. a. = not applicable.

	Prok ab	Vir ab	FIC	VP	PHP	Oxygen	NO_3	PO_4	SiO_4	n
All depths										
Prok. abundance	n. a.	**0.72**	**–0.73**	0.44	**0.95**	**–0.76**	-	-	**–0.90**	42
HNALS	n. a.	–0.46	-	-	–0.49	-	-	-	0.45	42
HNAHS	n. a.	-	**0.75**	-	–0.44	**0.75**	**–0.61**	**–0.59**	0.41	42
LNA	n. a.	**0.52**	**–0.73**	-	**0.76**	**–0.76**	-	-	**–0.72**	42
Viral abundance	**0.72**	n. a.	**–0.57**	-	**0.73**	–0.46	-	-	**–0.62**	42
Vir HIGH	**0.65**	n. a.	-	0.45	**0.68**	–0.33	-	-	**–0.59**	42
VP-Ratio	n. a.	n. a.	**0.56**	**–0.50**	–0.37	**0.62**	–0.45	–0.42	-	42
FIC	**–0.61**	**-0.57**	n. a.	-	**–0.62**	**0.73**	-	-	**0.60**	19
VP	-	-	-	n. a.	**0.53**	-	**0.58**	-	-	19
Epipelagic										
Geographic dist.	-	-	-	-	-	-	**–0.93**	**–0.93**	**–0.93**	7
Mesopelagic										
Prok. abundance	n. a.	**0.89**	-	-	**0.93**	**–0.56**	-	-	**–0.82**	13
HNAHS	n. a.	**–0.82**	-	-	**–0.79**	**0.67**	-	-	-	13
Viral abundance	**0.89**	n. a.	-	-	**0.77**	-	-	-	**–0.77**	13
Geographic dist.	-	-	-	-	-	-	**–0.95**	**0.92**	-	
Bathypelagic										
Prok. abundance	n. a.	-	-	-	**0.73**	-	-	-	**–0.67**	16
HNAHS	n. a.	-	**0.76**	**0.74**	-	**0.69**	-	-	-	16
LNA	n. a.	-	**–0.76**	**–0.71**	**0.60**	-	-	-	-	16
Vir HIGH	**0.76**	n. a.	-	-	**0.59**	-	-	-	-	16
VP-Ratio	n. a.	n. a.	-	-	-	-	-	-	**0.67**	16
FIC	-	-	n. a.	-	-	**0.88**	**–0.88**	-	-	8
VP	-	-	-	n. a.	-	**0.79**	-	-	-	8
Geographic dist.	-	-	**–0.80**	-	-	**–0.68**	**0.91**	**0.92**	-	
Abyssopelagic										
Vir LOW	-	n. a.	-	-	**0.94**	-	-	-	-	6
Vir MED	-	n. a.	-	-	**–0.94**	-	-	-	-	6
Geographic dist.	-	-	-	-	-	-	**–0.94**	-	-	6

Table 7 Mantel statistics (r_M) comparing community composition of prokaryotes and viruses with each other. All possible combinations were calculated, only significant results are shown here (see also Table 3). Dashes indicate no significant relationship, $r_M > 0.5$ printed in bold. Arch fwd = *Archaea* forward, Arch rev = *Archaea* reverse, Bac fwd = *Bacteria* forward, Bac rev = *Bacteria* reverse, n. a. = not applicable

	***Archaea* reverse**	***Bacteria* reverse**	**CRA**	**OPA**	**n**
All depths					
Archaea forward	0.47	-	-	-	42
Bacteria forward	-	**0.77**	-	-	42
Epipelagic					
Bacteria forward	-	**0.64**	-	-	7
Mesopelagic					
Archaea forward	**0.63**	-	-	-	13
Bacteria forward	-	**0.73**	-	-	13
CRA	-	-	n. a.	0.38	13
Bathypelagic					
Archaea forward	0.43	-	-	-	16
Bacteria forward	-	**0.76**	0.24	-	16
Abyssopelagic					
Bacteria forward	-	**0.80**	-	0.38	6

Table 8 Mantel statistics (r_M), comparing community composition with other parameters at all depths and in the specific depth layers. All possible combinations were calculated, only significant results are shown here (see also Table 3). Prokaryotic and viral populations determined by flow cytometry were only considered over all depths, not in the particular depth layers. Dashes indicate no significant relationship, $r_M > 0.5$ printed in bold. Arch fwd=*Archaea* forward, Arch rev=*Archaea* reverse, Bac fwd=*Bacteria* forward, Bac rev=*Bacteria* reverse. For other abbreviations see Table 4.

	Arch fwd	Arch rev	Bac fwd	Bac rev	CRA	OPA	n
All depths							
Depth	0.13	0.22	0.31	0.29	0.29	0.21	42
Temperature	0.17	0.25	0.37	0.33	0.33	0.19	42
Salinity	0.18	0.32	0.36	0.32	0.33	-	42
Prok. abundance	0.19	0.18	0.39	0.26	0.33	0.23	42
HNALS	-	-	0.29	0.27	0.26	-	
HNAHS	-	-	-	-	-	0.26	
Viral abundance	0.29	-	0.39	0.29	0.34	-	42
Vir HIGH	-	-	0.26	-	0.26	-	
VP-Ratio	-	0.30	-	-	-	-	42
Oxygen	-	-	-	-	-	0.18	40
NO_3	0.21	-	0.30	0.27	0.30	-	42
NO_2	0.33	-	0.32	0.34	0.32	-	42
PO_4	0.20	-	0.32	0.28	0.31	-	42
SiO_4	-	-	0.18	0.34	0.25	-	42
PHP	0.23	-	0.38	0.33	0.33	-	42
Geographic distance	-	-	0.15	0.18	0.11	-	42
Epipelagic							
Temperature	-	-	-	-	-	**0.80**	7
Viral abundance	-	-	-	**0.70**	-	-	7
VP-Ratio	-	-	**0.66**	**0.81**	-	-	7
Mesopelagic							
NH_4	-	-	-	-	0.43	-	13
Geographic distance	-	-	-	-	0.30	-	13
Bathypelagic							
NH_4	-	-	-	-	-	0.38	16
Geographic distance	-	-	0.18	0.28	-	-	16
Abyssopelagic							
Depth	-	-	**0.76**	-	-	-	6
Salinity	-	-	-	**0.66**	-	-	6
VP	-	-	**0.71**	-	-	**0.82**	5
PO_4	-	-	-	-	-	**0.54**	6

Figures

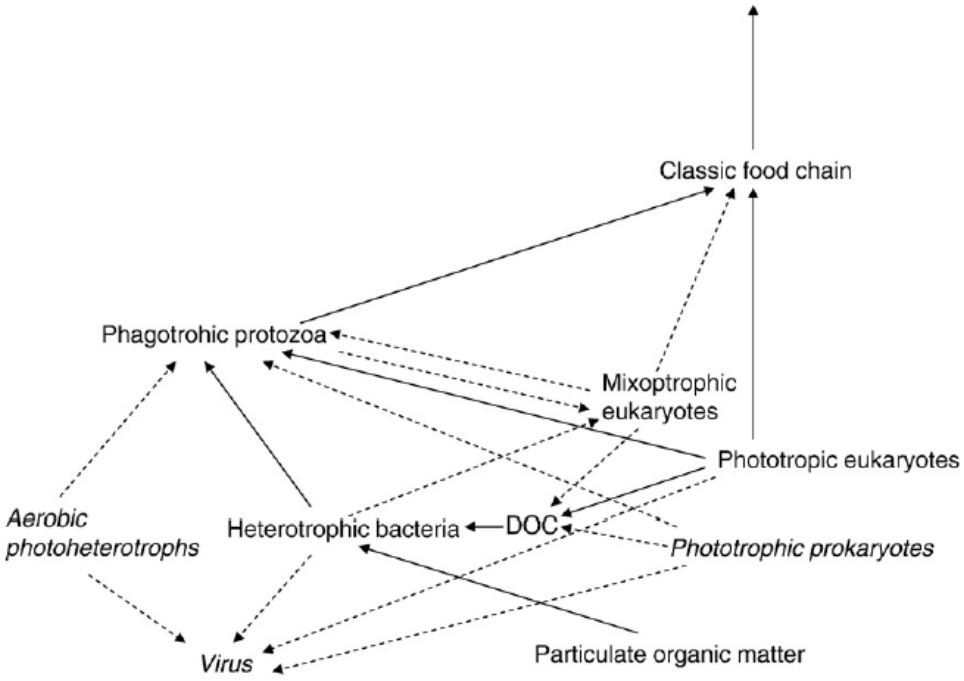

Figure 1 The microbial loop. Prokaryotes ("Heterotrophic bacteria") take up dissolved organic carbon (DOC) which derives from different sources. The prokaryotes are grazed by protozoans (e. g. ciliates and flagellates), and provide carbon for higher trophic levels in the classic food chain. Solid arrows depict the original concept of the microbial loop (Azam et al., 1983), dashed arrows show later additions. Taken from Fenchel (2008).

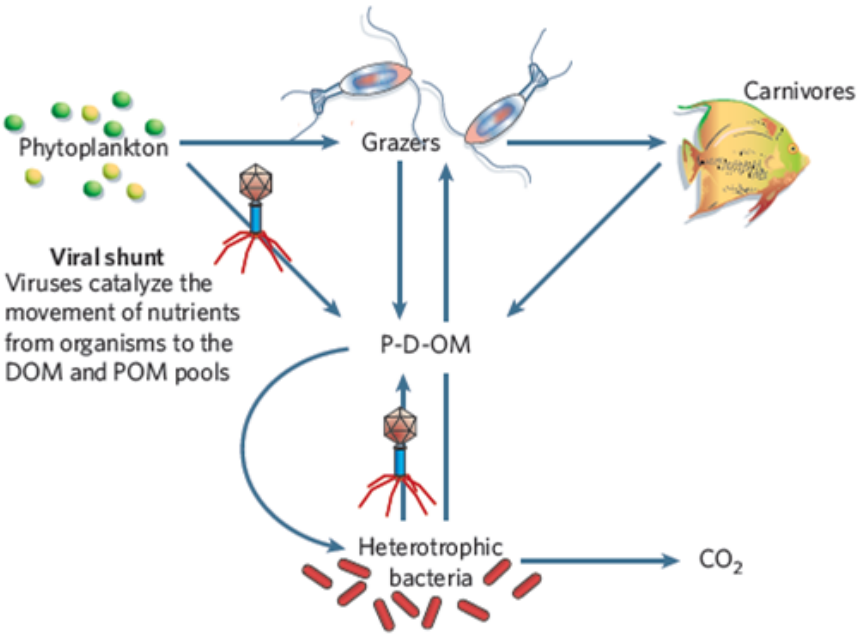

Figure 2 The viral shunt. Viruses convert single cell-organisms such as phytoplankton and prokaryotes ("Heterotrophic bacteria") into dissolved and particulate organic matter (P-D-OM), decreasing the trophic transfer efficiency of the marine foodweb.

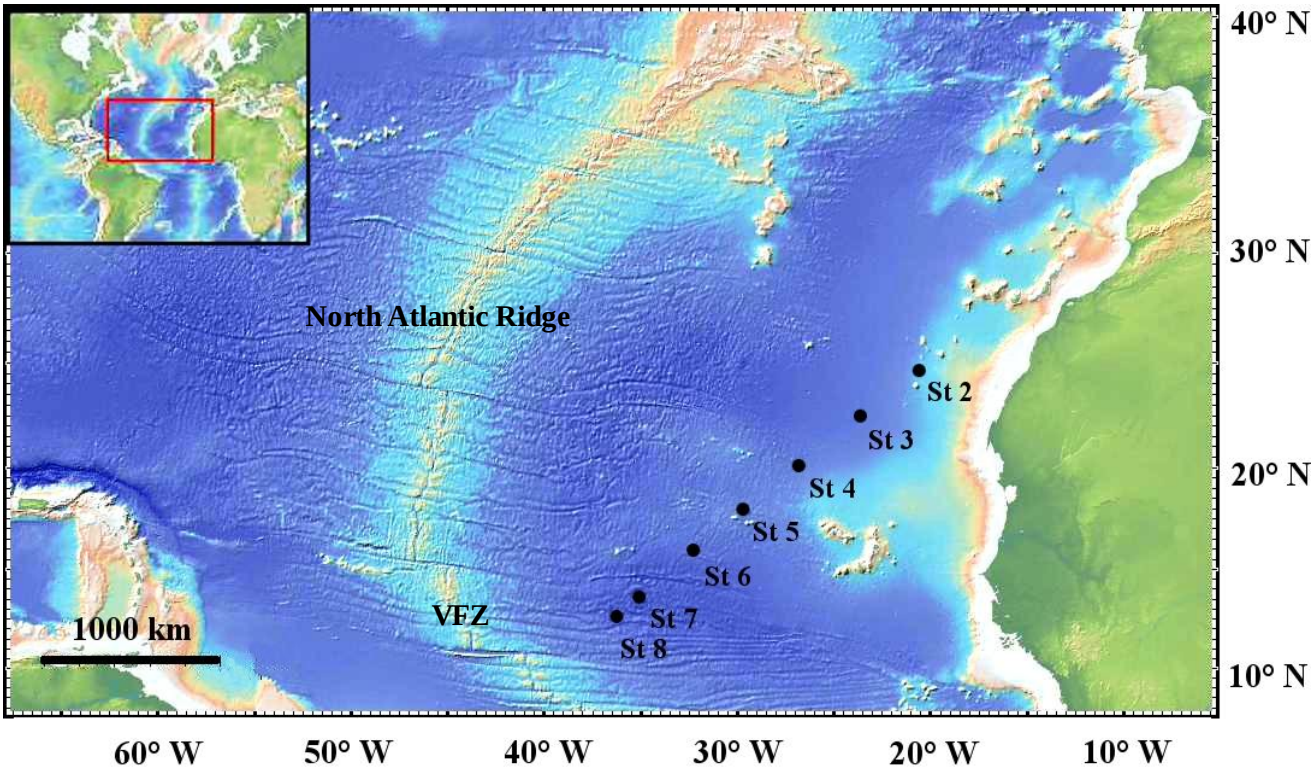

Figure 3 Map of the sampling stations in the subtropical Atlantic Ocean. Station 1 was a testing station. VFZ = Vema fracture zone. For exact positions of the stations see Table 1.

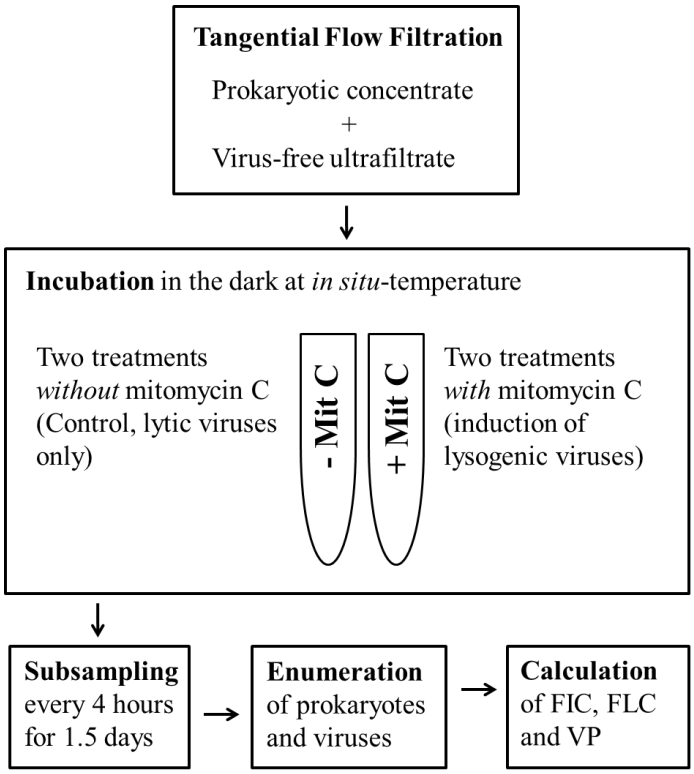

Figure 4 Schematic overview of the virus dilution approach. Tangential Flow Filtration, incubation and subsampling were performed on the R/V Pelagia. Enumeration and further processing the data was performed at the Department of Marine Biology, Vienna.

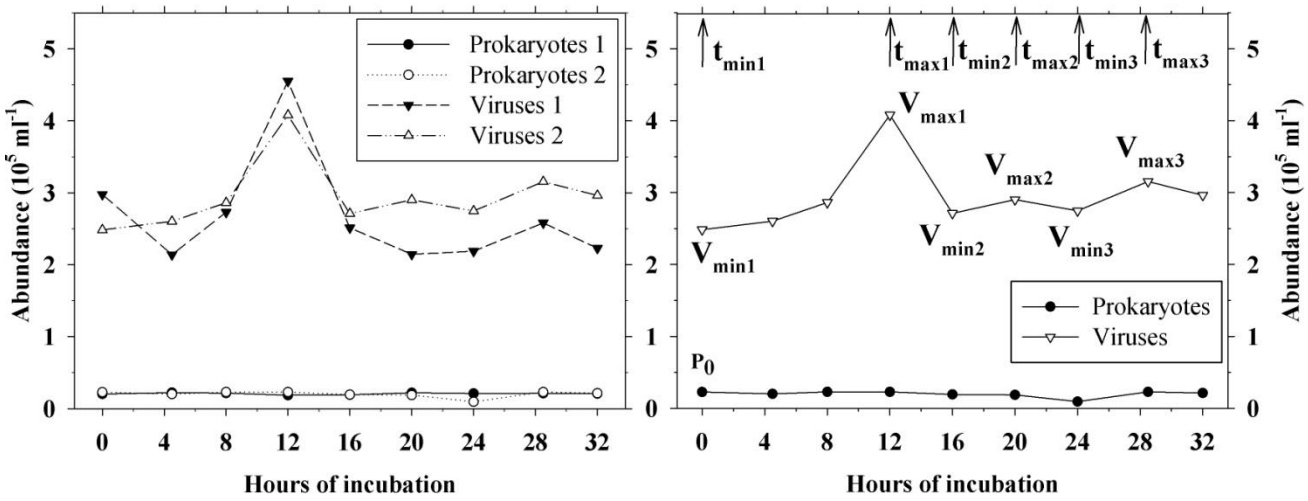

Figure 5 Example for a time course of prokaryotic and viral abundance over the 32 hours incubation period of the virus dilution experiment. Left: Duplicate treatments without Mitomycin C. Right: Illustration for calculating FIC and VP showing 3 lysis events in terms of peaks of viral abundance. Only one time course of the duplicate incubations is visible. P_0 = prokaryotic abundance at the beginning of incubation, V_{min} = viral abundance at low point, V_{max} = viral abundance at a peak, t_{min} = time at low point, t_{max} = time point at a peak. Station 2, 11 October 2010 at 3900 m depth, treatments without Mitomycin C.

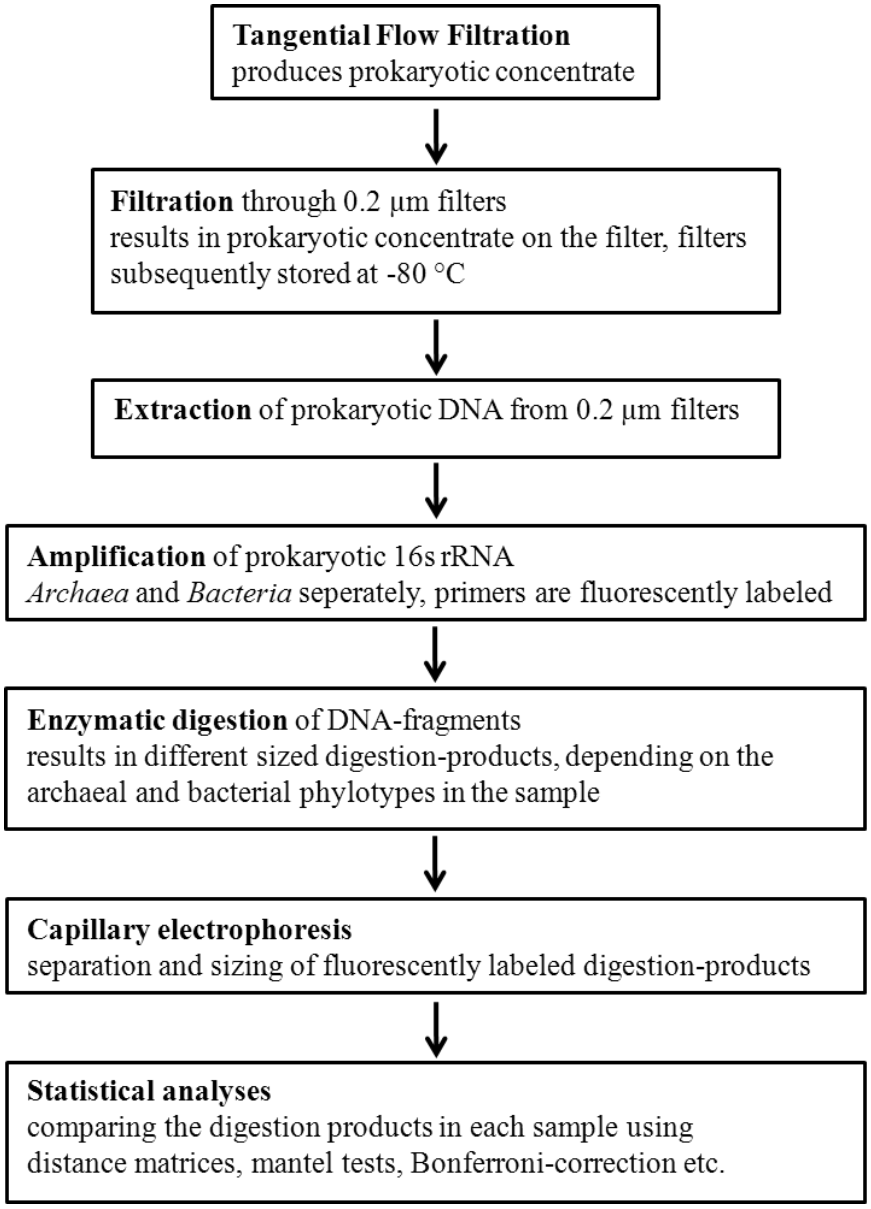

Figure 6 Schematic overview of the specific steps of T-RFLP. Tangential Flow Filtration and filtration through 0.2 µm-filters were performed on the ship, subsequent steps were performed in Vienna.

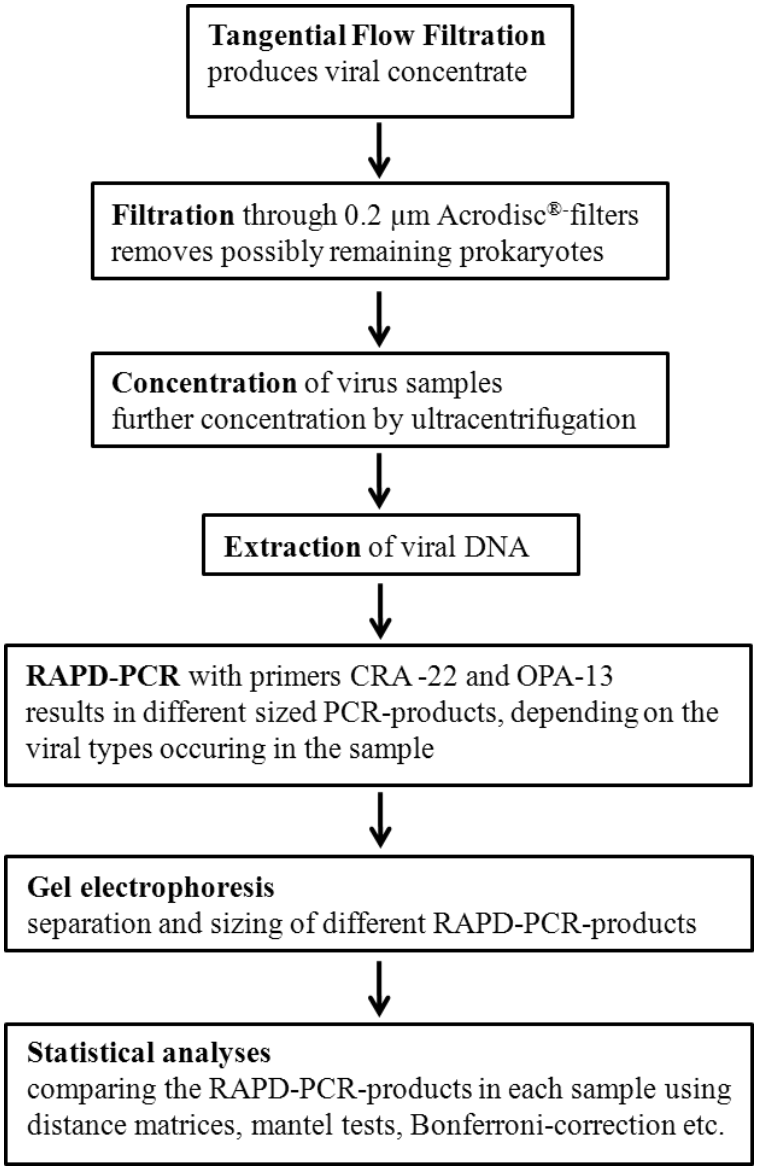

Figure 7 Schematic overview of the specific steps of RAPD-PCR. Tangential Flow Filtration was performed on the ship, filtration through 0.2 µm-filters and subsequent steps were performed in Vienna.

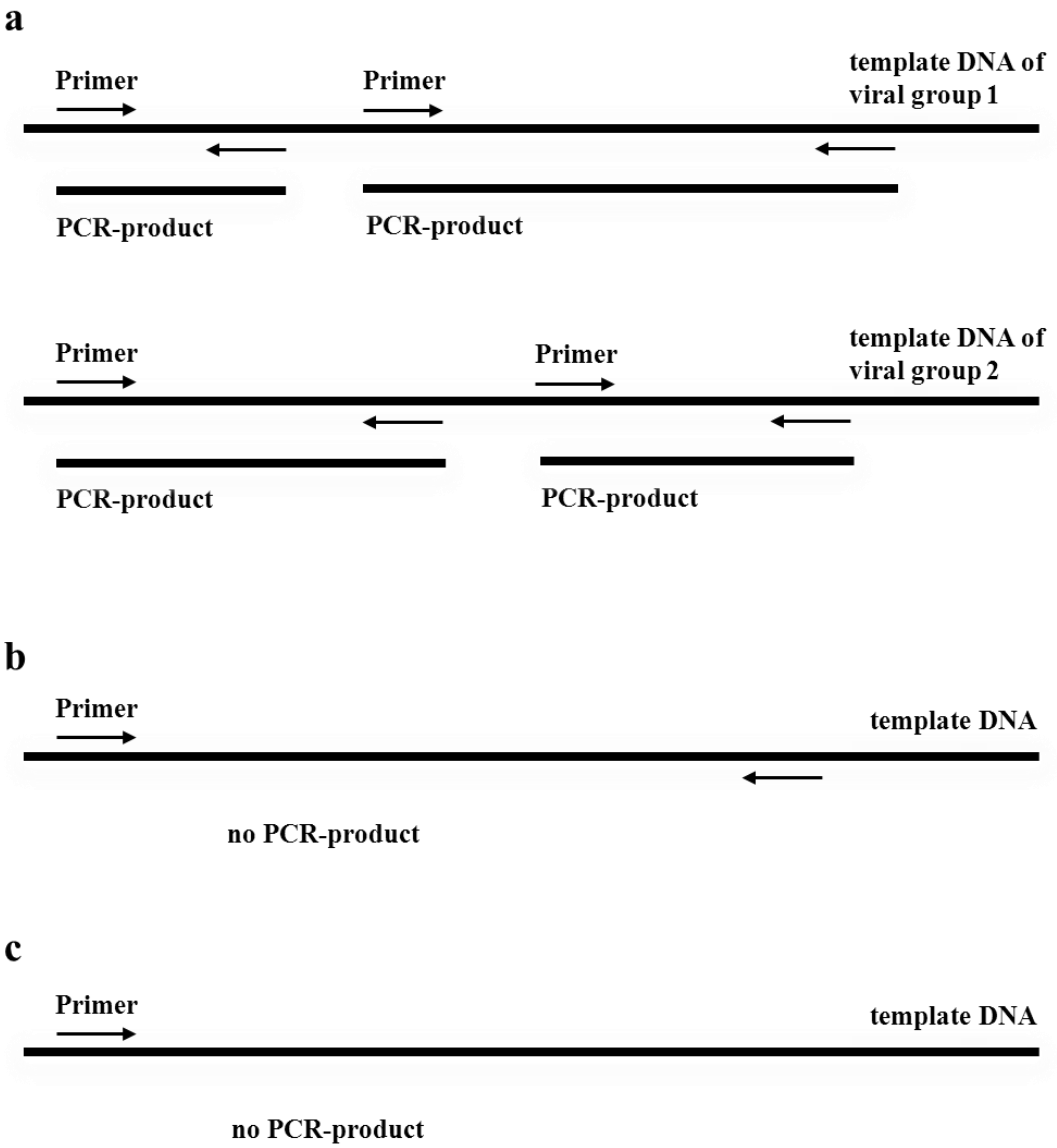

Figure 8 Schematic representation of the amplification in RAPD-PCR. Arrows represent primers with the same sequence, binding to priming sites on the template DNA. (a) PCR-products are formed since the primer-pair attaches to the template DNA pointing to each other and within a certain distance. Deviations in the sequences of different viral groups lead to different-sized PCR-products and allow their comparison. (b) Although the two primers are pointing toward each other, no PCR-product is formed because the primers are too far apart. (c) No PCR-product is formed since only one priming site occurred, but not the corresponding second one.

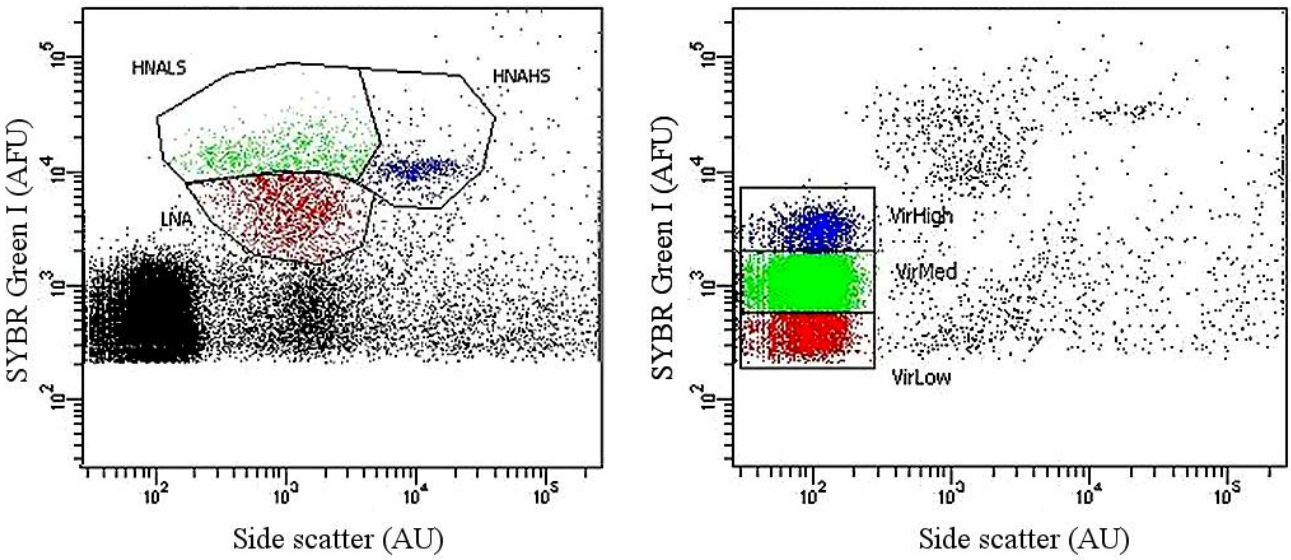

Figure 9 Gating of prokaryotic (left) and viral (right) populations based on SYBR Green fluorescence (arbitrary fluorescence units, AFU) and side scatter intensity (arbitrary units, AU). LNA = low nucleic acid prokaryotes, HNALS = high nucleic acid low side scatter prokaryotes, HNAHS = high nucleic acid high side scatter prokaryotes. VirLow, VirMed, VirHigh = low, medium and high fluorescent viruses, respectively.

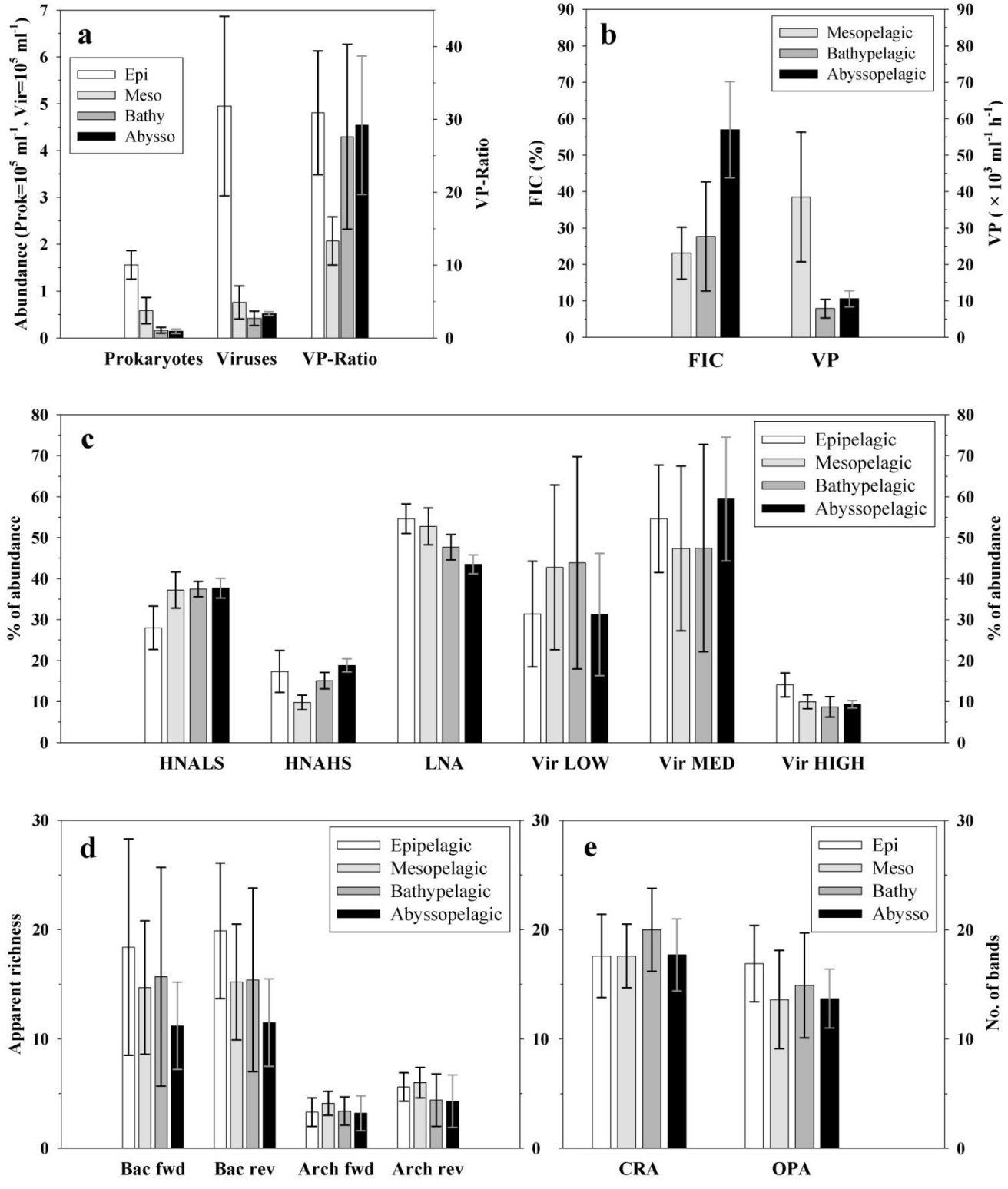

Figure 10 Parameters of all stations in the four depth layers. (a) Prokaryotic abundance, viral abundance and Virus-to-Prokaryote-Ratio (VP-Ratio). Note that the unit of prokaryotes is $\times 10^5$ ml^{-1} and that of viruses $\times 10^6$ ml^{-1}. (b) Frequency of infected cells (FIC) and viral production (VP). (c) Percentage of prokaryotic and viral populations distinguished by flow cytometry. (d) Apparent richness of prokaryotes (Number of T-RFLP peaks). (e) Number of bands determined by RAPD-PCR. For other abbreviations see Table 4.

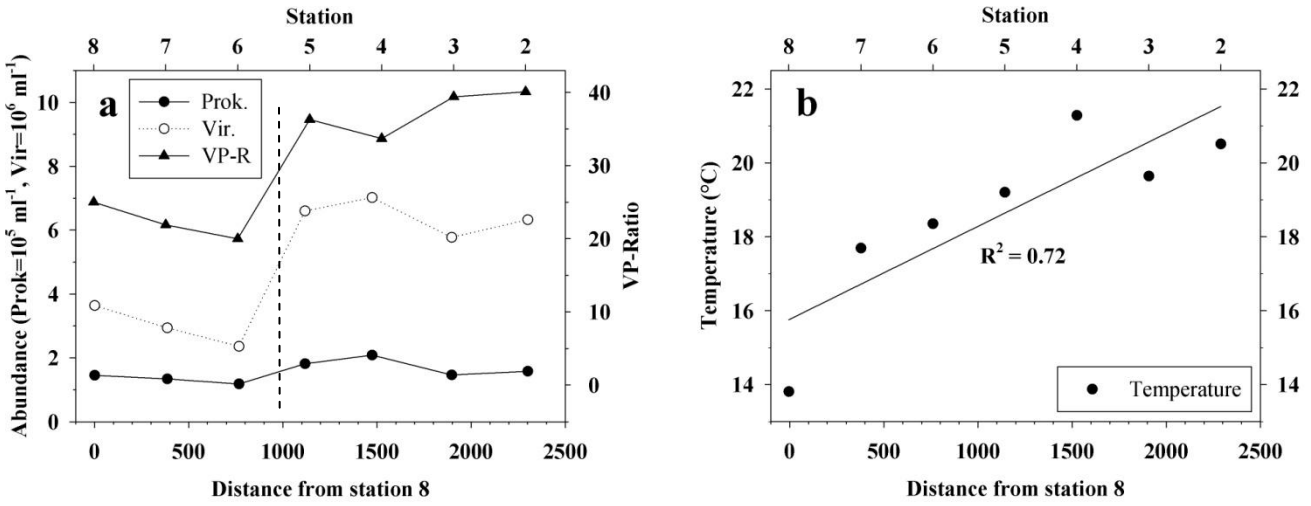

Figure 11 Selected parameters in the epipelagic compared over geographic distance. (a) Abundance of prokaryotes (Prok.), viruses (Vir.) and VP-Ratio (VP-R). (b) Temperature y = -0.96x + 23.45. Dashed line indicates arbitrary grouping of stations to compare difference of means by *t*-test or difference of medians by Mann-Whitney-test.

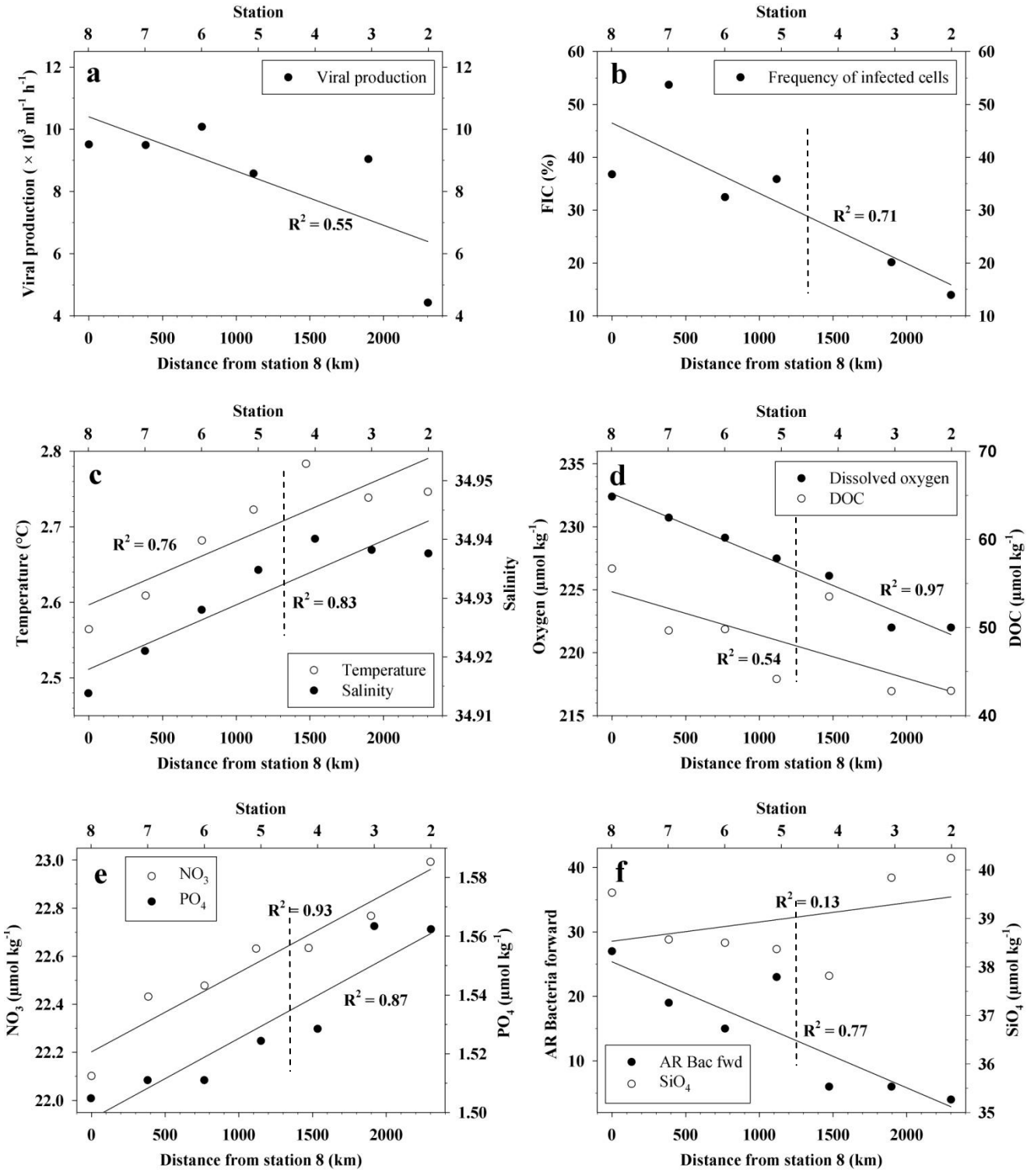

Figure 12 Lower North Atlantic Deep Water (sampled at ca. 3000 m depth). Selected parameters compared over geographic distance. (a) Viral production $y = -0.0017x + 10.40$ (b) Frequency of infected cells $y = -0.013x + 46.48$ (c) Temperature $y = 0.00008x + 2.60$; Salinity $y = -0.0042x + 34.95$ (d) Dissolved oxygen $y = -0.0049x + 232.64$ (e) Nitrate $y = -0.00033x + 22.20$; Phosphate $y = -0.011x + 1.58$ (f) Bacterial apparent richness (forward primer) $y = -0.0098x + 25.37$; Silicate $y = 3.97x + 38.53$. Dashed line indicates arbitrary grouping of stations to compare difference of means by *t*-test or difference of medians by Mann-Whitney-test.

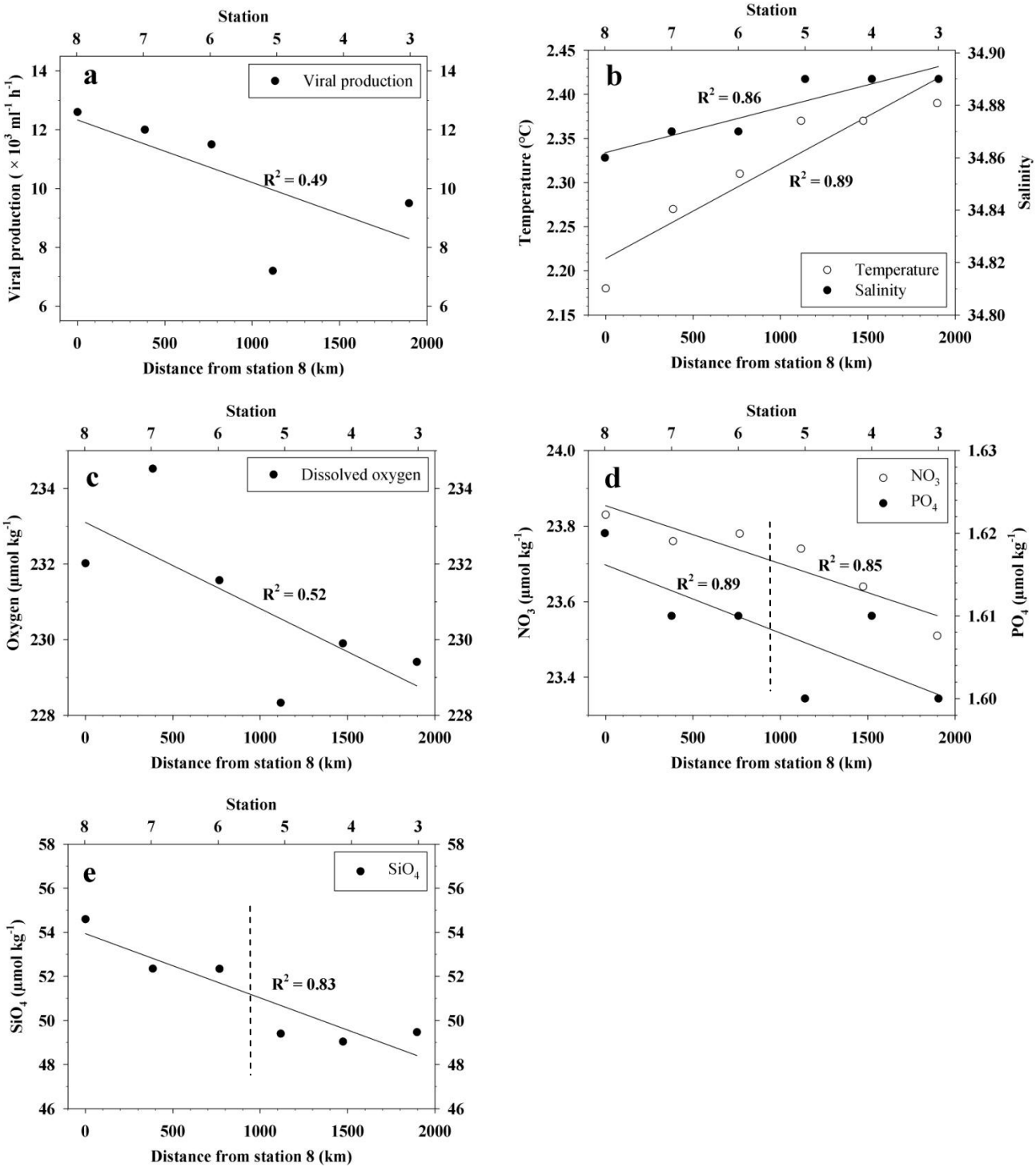

Figure 13 Abyssopelagic (Antarctic Bottom Water). Selected parameters compared over geographic distance. (a) Viral production $y = -0.0021x + 12.33$ (b) Temperature $y = -0.00011x + 2.21$; Salinity $y = -0.0066x + 34.91$ (c) Dissolved oxygen $y = -0.0023x + 233.10$ (d) Nitrate $y = 0.057x + 23.40$; Phosphate $y = 1.07x + 2.21$ (e) Silicate $y = -0.0029x + 53.94$. Dashed line indicates arbitrary grouping of stations to compare difference of means by *t*-test or difference of medians by Mann-Whitney-test.

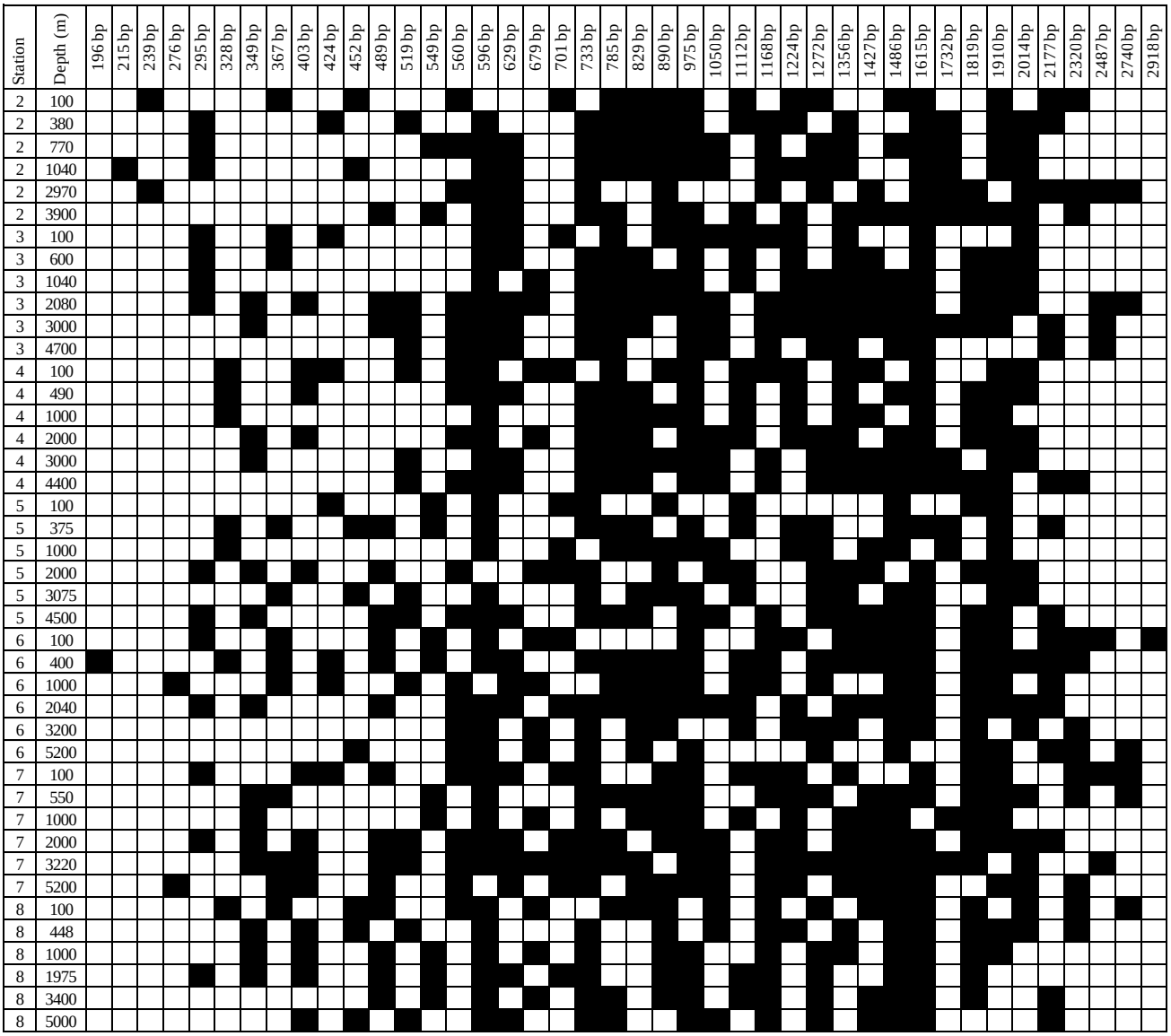

Figure 14 Example of viral community composition in form of a presence/absence matrix derived from RAPD-PCR performed with the primer CRA-22. Filled squares indicate presence, empty squares represent absence of a specific band for each sample.

Zusammenfassung

Die Bedeutung von Prokaryoten und deren Viren für biogeochemische Kreisläufe in marinen Ökosystemen wurde in den 1980er Jahren entdeckt. Prokaryoten (*Archaea* und *Bacteria*) nehmen gelöstes, organisches Material (engl. dissolved organic carbon = DOC) auf und führen es somit höheren trophischen Levels im Nahrungsnetz zu ("microbial loop"). Viren lysieren Prokaryoten (lytischer Zyklus) oder sie integrieren ihre Erbsubstanz in das Wirtsgenom, wo der einzelne Virus als so genannter Prophage weiter existiert und durch Zellteilung an Tochterzellen weitergegeben wird (lysogener Zyklus). Beim lytischen Zyklus wird DOC freigesetzt, welches somit verfügbar wird für andere Prokaryoten, man nennt diesen Mechanismus „viral shunt". Der lysogene Zyklus hingegen scheint unter Bedingungen niedriger Wirtsabundanz und -aktivität bevorzugt zu werden, kann aber zum lytischen Zyklus wechseln, wenn sich die Bedingungen ändern bzw. wenn es von außen induziert wird. Im Rahmen der MOCA cruise im Oktober 2010 wurden Proben an 7 Stationen mit jeweils 6 unterschiedlichen Tiefenstufen genommen und mithilfe von Inkubationsexperimenten, Flow Cytometer und molekularbiologischen Methoden untersucht. Dabei wurden u. A. Abundanzen von Prokaryoten und Viren, lytic viral production (VP), frequency of infected cells (FIC) und frequency of lysogenic cells (FLC) ermittelt. Zusätzlich wurde terminal restriction fragment length polymorphism (T-RFLP) und randomly amplified polymorphic DNA-PCR (RAPD-PCR) durchgeführt, um Prokaryoten bzw. Viren zu charakterisieren und die unterschiedlichen Stationen und Tiefen hinsichtlich ihrer Zusammensetzung miteinander zu vergleichen. Andere Parameter, welche im Zuge der Cruise ermittelt wurden, wie beispielsweise prokaryotic heterotrophic production (PHP), Sauerstoff- und Nährstoffkonzentrationen, Temperatur etc. wurden ebenfalls in die Auswertung miteinbezogen. Rangkorrelationen, Vergleiche der 4 Tiefenstufen mittels *t*- bzw. Mann-Whitney-test sowie Mantel tests wurden berechnet. Wie erwartet, nahmen die Abundanzen von Prokaryoten und Viren an jeder Station mit zunehmender Tiefe exponentiell ab, weiters waren beide miteinander positiv korreliert. Die Anzahl an Viren schwankte stärker als die Anzahl der Prokaryoten, was darauf hinweist, dass virale Abundanz einer nicht so engen Kontrolle unterworfen ist. Der Grund für die entdeckte Zunahme von FIC mit der Wassertiefe könnte eine geringere Zahl an Protisten in der Tiefe sein. VP korrelierte positiv mit der Anzahl an Prokaryoten und mit PHP, da eine höhere Zahl aktiver Zellen mehr Viren produzieren können. Von den verschiedenen Gruppen, die am Flow Cytometer hinsichtlich Fluoreszenz unterschieden werden können, waren Prokaryoten mit geringem Nukleinsäureanteil (LNA) positiv korreliert mit PHP. Dies weist darauf hin, dass LNA-Prokaryoten einen wichtigen Beitrag zur PHP in oligotropher, offener See leisten. Am häufigsten waren Viren mit mittlerer Fluoreszenz (Vir MED), welche auch in anderen Studien sehr

zahlreich in der pelagischen Tiefsee waren. Im Gegensatz dazu scheinen Viren mit niedriger Fluoreszenz (VirLOW) in Küstenregionen zu dominieren. Sowohl die mikrobiellen Gemeinschaften von Prokaryoten als auch jene von Viren scheinen sich stärker bezüglich Tiefe zu unterscheiden als hinsichtlich geographischer Distanz. Da die apparent richness (AR) von Prokaryoten und die Anzahl viraler RAPD-PCR Banden über die Tiefe hinweg mehr oder weniger konstant bleibt, weist dies auf eine Änderung der Artenzusammensetzung bei einer gleichbleibenden Anzahl unterschiedlicher Taxa hin. Das Verhältnis von Prokaryoten zu Viren (VP-Ratio) korrelierte mit bakterieller AR, dies ist in Einklang mit der Auffassung, dass Viren eine hohe Vielfalt an *Bacteria* aufrechterhalten. VP, FIC, Temperatur, Salinität, Sauerstoff und anorganische Nährstoffe (Nitrat, Phosphat) ändern sich in den tiefsten untersuchten Wassermassen (ca. 3000 bis 5200 m) mit zunehmender Distanz der einzelnen Probestationen. Dies weist darauf hin, dass der Eintrag von sauerstoffreichen Wassermassen (LNADW, AABW) vom westlichen ins östliche Becken durch die Vema Fracture Zone (VFZ) einen Effekt auf mikrobielle und virale Gemeinschaften hat.

Summary

The importance of prokaryotes and their viruses for biogeochemical cycling in marine environments was discovered in the 1980s. Prokaryotes (*Archaea* and *Bacteria*) take up dissolved organic carbon (DOC) and make it available for higher trophic levels of the food web ("microbial loop"). Viruses infecting prokaryotes either lyse their hosts (lytic cycle) or integrate into the host genome, where they are passed on to daughter cells (lysogenic cycle). Through viral lysis, DOC is released, which is then available for other prokaryotes, a mechanism called "viral shunt". Lysogeny, on the contrary, is considered to be favored under conditions of low host abundance and activity and can switch to the lytic cycle again, when the conditions change. During the MOCA cruise in October 2010, samples were taken from 7 stations and depth layers and analyzed using incubation experiments and flow cytometry to gain knowledge about the abundance of prokaryotes and viruses, lytic viral production (VP), frequency of infected cells (FIC), frequency of lysogenic cells (FLC) and other parameters. In addition, terminal restriction fragment length polymorphism (T-RFLP) and randomly amplified polymorphic DNA-PCR (RAPD-PCR) were performed to fingerprint and to compare prokaryotic and viral communities, respectively. Other parameters determined aboard the ship such as prokaryotic heterotrophic production (PHP), oxygen and nutrient concentrations, temperature, etc. were also taken into account and rank correlation statistics, comparison of 4 different depth layers as well as mantel tests were carried out. As expected, prokaryotic and viral abundance decreased

exponentially with depth and correlated positively with each other at all stations. The number of viruses shows higher variability, suggesting that viral abundance is less tightly controlled than prokaryotic abundance. The reason for the discovered increase of FIC with depth could be the occurrence of fewer predators in deeper waters. Moreover, the more prokaryotes that were infected, the lower their production, since viruses could influence the activity of their hosts. VP is positively linked to prokaryotic abundance and PHP, since more active cells can produce more viruses. From different populations distinguished by flow cytometry, prokaryotes with low nucleic acid-content (LNA) were correlated to PHP, suggesting that LNA-prokaryotes are important drivers of PHP in oligotrophic, open ocean. Medium fluorescence viruses (Vir MED) were most abundant, they were found in other studies to be dominant in pelagic, deep waters, whereas viruses with low fluorescence (Vir LOW) appear to dominate in coastal regions. The composition of both viral and prokaryotic communities seem to be stronger influenced by depth than by geographic distance. Since apparent richness (AR) of prokaryotes and number of viral bands at the same time remains more or less constant over depth, this indicates a potential shift of the communities with a constant number of different types of prokaryotes and viruses. The virus-to-prokaryote-ratio (VP-Ratio) is correlated to AR of *Bacteria*, suggesting that viruses maintain host diversity. The deepest investigated water layers (ca. 3000 to 5200 m) show some distinct patterns of change of specific parameters such as VP, FIC, temperature, salinity, oxygen and inorganic nutrients over geographic distance, indicating an effect on microbial and viral communities by input of oxygen-rich water from the western Atlantic basin through the Vema Fracture Zone (VFZ).

THOMAS GRIESSLER

born on 7th November 1980 in Scheibbs/Lower Austria

EDUCATION

1987 - 1991	Elementary School	Kirnberg / Mank
1991 - 1995	Secondary Modern School	Mank
1995 - 1999	Technical School - civil engineering	Krems / Donau
2001 - 2004	Resuming technical school Krems, school leaving examination	Krems / Donau
since 2006	Studies in Biology/Zoology / Marine microbial Ecology	University of Vienna, University of Lund, Sweden

WORK EXPERIENCE

1999 - 2001	Technician - landscape architecture / GIS	Loosdorf
2003, 2004	Archaeological work - Bronze Age-excavations	St. Pölten
2005 - 2006	Technician - construction business	Vienna
2006	Different jobs in building stages, light & sound	Vienna
2007, 2008	Part time job as a restauration joiner	Vienna
2007, 2008	Audience service at Wiener Festwochen	Vienna
2008, 2009	Project work at the Konrad Lorenz Institute for Ethology	Vienna
2009	Project work at the Ludwig Boltzman Institute for Traumatology	Vienna
2011	Tutor for animal morphology course at University	University of Vienna
2011 - 2012	Diveguide	Panglao, Philippines

SKILLS

- Good computer skills: Office, statistics, image processing etc.
- Technical and manual experience and knowledge
- Lab experience
- PADI Divemaster

INTERESTS

Diving, Science, Photography, Music, Friends etc.